PRODUCTION OF PERSONALIZED AORTIC VALVE WITH 3D BIOPRINTING

A THESIS SUBMITTED TO
THE GRADUATE SCHOOL OF NATURAL AND APPLIED SCIENCES
OF
ANKARA UNIVERSITY

by

Utku Serhat DERİCİ

IN PARTIAL FULFILMENT OF THE REQUIREMENTS
FOR THE DEGREE OF
MASTER OF SCIENCE
IN
BIOMEDICAL ENGINEERING

ANKARA
2025

All rights reserved

ABSTRACT

Master's Thesis

PRODUCTION OF PERSONALIZED AORTIC VALVE WITH 3D BIOPRINTING

Utku Serhat DERİCİ

Ankara University
Graduate School of Natural and Applied Sciences
Department of Biomedical Engineering

Supervisor: Prof. Dr. Pınar YILGÖR HURİ

This thesis investigates the creation of biomimetic aortic valve equivalents through advanced 3D bioprinting technologies, emphasizing personalized tissue-engineered approaches for heart valve diseases. Dual-phase scaffolds were fabricated by integrating thermoplastic polyurethane (TPU) with GelMA/gelatin-based hydrogels to mimic the properties of natural aortic valves. The tissue scaffolds were augmented with controlled-release systems that deliver VEGF and TGF-β1, thereby facilitating cell proliferation and differentiation. Adipose-derived stem cells (ASCs) were cultured on the TPU/GelMA scaffolds to review their biocompatibility, viability, and regenerative potential. Mechanical testing validated the scaffolds' capacity to endure physiological pressures, and cytotoxicity assessments indicated their safety. Optimized bioink formulations achieved precise structural and functional fidelity, allowing the scaffolds to replicate the anisotropic mechanics of native valve tissue. In vitro experiments conducted over 14 days demonstrated the efficacy of VEGF and TGF-β1 in promoting ASC proliferation and extracellular matrix formation and differentiation. The findings demonstrate that these engineered valves address the shortcomings of traditional heart valve replacements, including limited growth potential and the risk of immune rejection. This study provides a foundational framework for preclinical research, applicable to both pediatric and adult patient populations in need of long-term, adaptive valve solutions. This thesis integrates innovative biomaterials, stem cell technology, and advanced biofabrication techniques, thereby advancing the regenerative cardiovascular medicine field. The results indicate viability of developing living, functional, and patient-specific aortic valves, presenting a promising alternative to existing clinical methods and facilitating future progress in personalized therapeutic approach.

January 2025, 71 pages

Key Words: Aortic Valve; Tissue Engineering; Stem Cell; Cell Culture; Biomaterials

ÖZET

Yüksek Lisans Tezi

3B BİYOBASKILAMA İLE KİŞİSELLEŞTİRİLMİŞ AORT KAPAK ÜRETİMİ

Utku Serhat DERİCİ

Ankara Üniversitesi
Fen Bilimleri Enstitüsü
Biyomedikal Mühendisliği Anabilim Dalı

Danışman: Prof. Dr. Pınar YILGÖR HURİ

Bu tez, kalp kapakçığı hastalıkları için kişiselleştirilmiş doku mühendisliği yaklaşımlarını vurgulayarak, gelişmiş 3D biyobaskılama teknolojileri aracılığıyla biyomimetik aort kapak eşdeğerlerinin oluşturulmasını araştırmaktadır. Doğal aort kapakçıklarının mekanik ve biyolojik özelliklerini taklit etmek için termoplastik poliüretan (TPU) ile GelMA/jelatin bazlı hidrojellerin entegre edilmesiyle çift fazlı iskeleler üretilmiştir. İskeleler, VEGF ve TGF-β1 sağlayan kontrollü salım sistemleriyle desteklenmiştir, böylece hücre çoğalması ve farklılaşması kolaylaştırılmıştır. Biyouyumluluklarını, canlılıklarını ve rejeneratif potansiyellerini değerlendirmek için yağdan türetilen kök hücreler (ASC'ler) iskeleler üzerinde kültürlenmiştir. Mekanik testler, iskelelerin fizyolojik basınçlara dayanma kapasitesini doğrulamış ve sitotoksisite değerlendirmeleri bunların güvenliğini göstermiştir. Optimize edilmiş biyomürekkep formülasyonları, iskelelerin doğal kapak dokusunun anizotropik mekaniğini taklit etmesine olanak tanıyan hassas yapısal ve işlevsel özellikler elde etmiştir. 14 gün boyunca yürütülen in vitro deneyler, VEGF ve TGF-β1'in ASC proliferasyonunu ve hücre dışı matris oluşumunu desteklemedeki etkinliğini göstermiştir. Bulgular, bu tasarlanmış kapakların sınırlı büyüme potansiyeli ve bağışıklık reddi riski dahil olmak üzere geleneksel kalp kapakçığı replasmanlarının eksikliklerini ele aldığını göstermektedir. Bu çalışma, uzun vadeli, adaptif kapak çözümlerine ihtiyaç duyan hem pediatrik hem de yetişkin hasta popülasyonlarına uygulanabilen klinik öncesi araştırmalar için temel bir çerçeve sunmaktadır. Bu tez, yenilikçi biyomalzemeleri, kök hücre teknolojisini ve gelişmiş biyofabrikasyon tekniklerini birleştirerek rejeneratif kardiyovasküler tıp alanını ilerletmektedir. Sonuçlar, canlı, işlevsel ve hastaya özgü aort kapakçıkları geliştirmenin uygulanabilirliğini göstermekte, mevcut klinik yöntemlere umut verici bir alternatif sunmakta ve kişiselleştirilmiş terapötik yaklaşımlarda gelecekteki ilerlemeyi kolaylaştırmaktadır.

Ocak 2025, 71 sayfa

Anahtar Kelimeler: Aort Kapağı; Doku Mühendisliği; Kök Hücre; Hücre Kültürü; Biyomalzemeler

FOREWORD AND ACKNOWLEDGEMENTS

First and foremost, I would like to express my deepest gratitude to my advisor, Prof Dr. Pınar YILGÖR HURİ, for their unwavering guidance, encouragement, and invaluable support throughout my MSc journey. Their expertise and thoughtful mentorship have been pivotal in shaping my understanding of the subject and inspiring me to push beyond my boundaries. Their patience and dedication have not only helped me navigate the challenges of this research but also taught me the value of perseverance and intellectual curiosity.

I am profoundly thankful to the members of my lab group, whose collaboration and support have been essential throughout this process. Working alongside such talented and passionate individuals has been a truly enriching experience. The shared moments of learning and laughter have made this journey both productive and enjoyable, and I am honored to have been part of this dynamic team.

I am also deeply indebted to my family, who have been my greatest source of strength and motivation. Their unwavering support, encouragement, and sacrifices have made this achievement possible. Their constant love and guidance have provided me with the confidence and determination to pursue my goals.

Finally, I would like to extend my appreciation to everyone who has supported me in both direct and indirect ways during my MSc studies. Whether through academic discussions, friendship, or simply being there when I needed encouragement, your presence has meant more than words can express. I carry the lessons and memories from this experience with me as I move forward.

This thesis is the result of the collective efforts, support, and inspiration of all these wonderful individuals, and I dedicate it to each one of them. Thank you for believing in me and making this journey so fulfilling.

Utku Serhat DERİCİ
Ankara, January 2025

TABLE OF CONTENTS

SYMBOLS AND ABBREVIATIONS

3D	Three-Dimensional
AM	Additive Manufacturing
AR	Aortic Regurgitation
AS	Aortic Stenosis
ASC	Adipose-derived Stem Cells
CDDS	Controlled Drug Delivery Systems
DCM	Dichloromethane
DMEM	Dulbecco's Modified Eagle Medium
DMSO	Dimethyl Sulfoxide
ECM	Extracellular Matrix
EGF	Epidermal Growth Factor
ESC	Embryonic Stem Cells
FBS	Fetal Bovine Serum
FDM	Fused Deposition Method
FGF	Fibroblast Growth Factor
GelMA	Gelatin Methacrylate
GF	Growth Factor
HCL	Hydrochloric Acid
P/S	Penicillin/Streptomycin
PBS	Phosphate Buffer Saline
PCL	Poly(ε-caprolactone)
PEG	Poly(ethylene) Glycol
PGA	Poly(glycolic) Acid
PLA	Polylactic Acid

PLGA	Poly(lactic-co-glycolic) Acid
PFA	Paraformaldehyde
PVA	Polyvinyl Alcohol
SEM	Scanning Electron Microscopy
SLA	Stereolithography
SLS	Selective Laser Sintering
SSC	Somatic Stem Cells
TE	Tissue Engineering
TGF-β	Transforming Growth Factor Beta
TEHVs	Tissue-engineered heart valves
THF	Tetrahydrofuran
TPU	Thermoplastic Polyurethane
VEGF	Vascular Endothelial Growth Factor

LIST OF FIGURES

LIST OF TABLES

1. INTRODUCTION

This thesis focused on designing three-dimensional (3D) scaffolds integrated with a controlled growth factor delivery system to support the in vitro development of aortic heart valves from a single stem cell source. Such a system holds the potential to greatly enhance outcomes for geriatric and pediatric patients requiring custom-designed heart valves in the future.

1.1 Structure of Aortic Valve Tissue

The aortic valve is a crucial cardiac component that facilitates unidirectional blood flow from the left ventricle to the aorta while inhibiting retrograde flow. The aortic valve consists of three slender but sturdy leaflets: the right coronary cusp, the left coronary cusp, and the non-coronary cusp. The nomenclature of these leaflets is dictated by their positioning relative to the apertures of the coronary arteries. The heart's pumping motion, despite its fragile nature, enables it to endure continuous mechanical stress. Three separate layers within each leaflet work together to regulate the pressures on the valve (Mosch et al., 2017). The inner layer, termed the ventricularis, comprises elastin fibers that confer the capacity to stretch and rapidly revert to shape when the valve operates (Figure 1.1). Proteoglycans and glycosaminoglycans constitute the softer, cushion-like spongiosa layer centrally located. This layer attenuates impact and offers flexibility. The outer layer, known as the fibrosa, is abundant in collagen fibers, providing the valve with the strength necessary to endure the high pressures of blood flow. The aortic annulus, a robust fibrous ring that preserves its form and supports its function, secures the valve. The sinuses of Valsalva, small pouch-like structures encircling the valve, facilitate blood flow and alleviate stress on the leaflets during closure. These sinuses are crucial for channeling blood into the coronary arteries that nourish the heart muscle. The intricate design of the aortic valve, characterized by its strength, flexibility, and resilience, exemplifies a remarkable feat of natural engineering (Yacoub & Takkenberg, 2005). This complexity renders it a significant focal point in tissue engineering research, as emulating its distinctive architecture is crucial for formulating successful therapies for valve disorders.

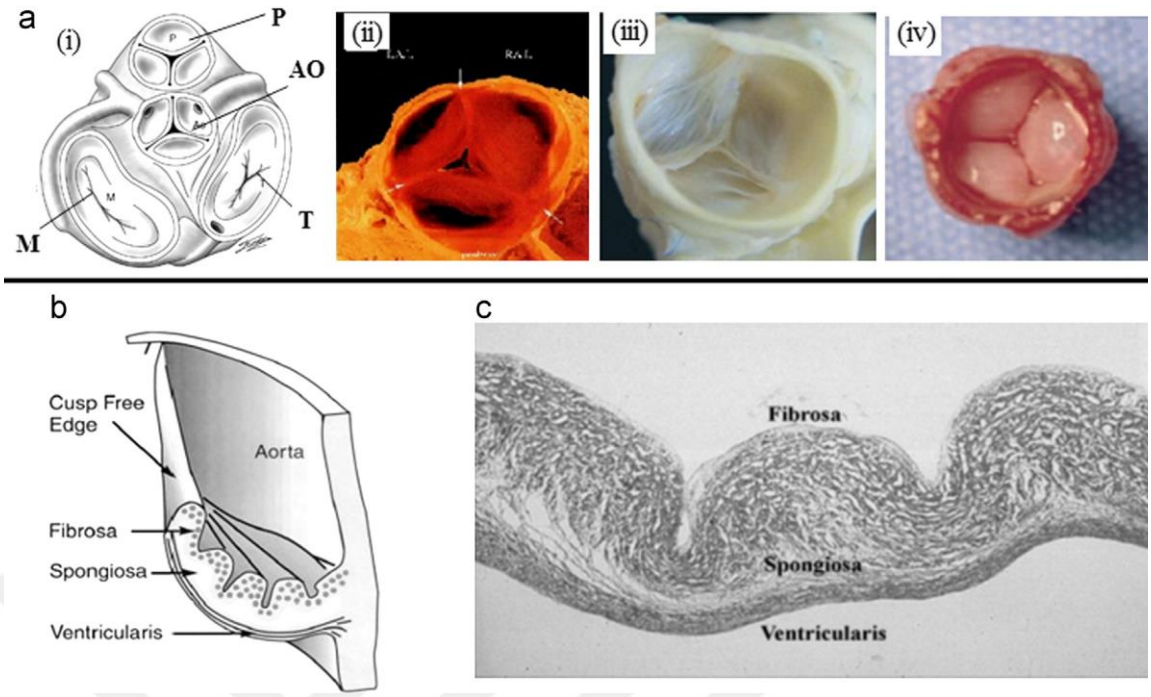

Figure 1.1 (a) Valve structure and composition, (b) illustration of layers of the aortic valve (c) histology of the aortic valve (Hasan et al., 2014)

1.2 Heart Valve Diseases

Valvular heart diseases rank as the third most significant cause of cardiovascular conditions, impacting over five million individuals in the United States and accounting for 3% of annual sudden deaths in the European Union (Wu et al., 2019). Globally, more than 290,000 valve replacement surgeries are performed annually, with this figure expected to rise to 850,000 by 2050 due to the aging population (Sewell-Loftin et al., 2011). Aortic valves are important for keeping blood flowing in the right direction from the left ventricle to the aorta, which helps to circulate blood efficiently in the body. Changes in the structure or function of this valve can seriously affect blood flow and lead to a range of issues known as aortic valve diseases (Mendoza et al., 2024). These conditions affect many people around the world, whether they are born with them or develop them later in life. Congenital malformations, like bicuspid aortic valves, are more common in younger people, whereas degenerative changes, such as calcific aortic stenosis, are more prevalent in older adults (Figliozzi et al., 2024). As aortic valve diseases become more common, especially in older populations, it's important to really grasp their underlying causes, risk factors, and how they are present in patients. Valve

leaflet calcification, endocarditis (which is the inflammation of the heart's inner lining), congenital valve anomalies, and heart valve dysfunction are the primary causes(Min and Cho S. W., 2022). The valves in the pulmonary and systemic circulations open in a way that allows blood to flow into the ventricles even when there's systolic pressure. In the aorta, with every heartbeat, certain areas of the valves undergo considerable changes and face intense shear stresses from the flowing blood (Hasan et al., 2014). Valve disease can happen in all of the valves, but Aortic Valve (AV) and Mitral Valve (MV) diseases are seen most often. Heart valves that are affected by disease show changes in the extracellular matrix (ECM) layer and have irregularities in the valvular interstitial cells (Fidalgo et al., 2018). The changes in structure affect how the heart valves work. When blood flow is restricted in one direction, it leads to stenosis, and these structural issues impact how the heart valves work, resulting in blood flowing backward (Rendon-Romero et al., 2024).

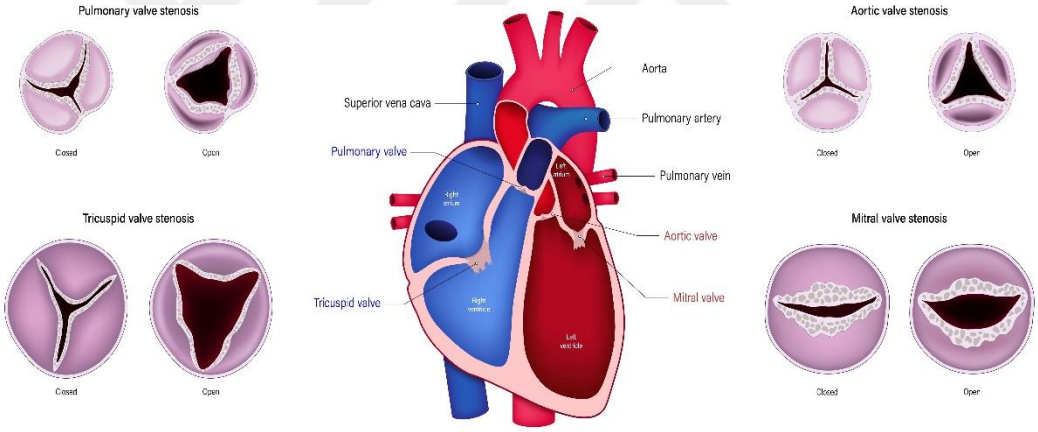

Figure 1.2 Heart valve diseases (Yadid et al., 2022)

Aortic stenosis happens when the opening of the aortic valve gradually narrows. There are several factors cause development of AS, with calcific degeneration being the most prevalent cause in developed countries, especially in older adults (Engin and Güvenç O., 2024). Rheumatic fever, while not as common in industrialized countries, still plays a major role in causing AS in developing areas. Congenital abnormalities like a bicuspid aortic valve affect about 1-2% of people and can lead to an earlier onset of aortic stenosis because of faster degeneration (Gao et al., 2024). AS pathophysiology is characterized by the gradual buildup of calcific nodules on the valve cusps, usually alongside inflammatory

processes and lipid infiltration. The changes result in a decreased movement of the leaflets, higher pressure gradients across the valve, and ultimately, left ventricular hypertrophy as a way for the heart to compensate (Nuche et al., 2024). Symptoms usually show up later in the disease and can include shortness of breath during activity, chest pain, and fainting. If left untreated, severe AS can lead to significant health issues and a higher risk of death (Figure 1.2).

Aortic regurgitation happens when the aortic valve doesn't shut completely during diastole. This condition can happen because of issues with the primary valve leaflets or as a result of the aortic root expanding, which affects how well the valve cusps come together (Ahmed et al., 2024). Acute aortic regurgitation is usually linked to issues like aortic dissection or infective endocarditis, whereas chronic aortic regurgitation is often related to connective tissue disorders, degenerative changes, or prolonged high blood pressure (Loshusan et al., 2024). In AR, the way the body works is affected by an overload of volume in the left ventricle. This situation causes the ventricle to gradually stretch and enlarge, resulting in a change in its shape and size. As time goes on, this compensatory mechanism starts to break down.

1.3 Methods for Aortic Valve Repair or Replacement

Aortic valve repair and replacement are important procedures for treating aortic valve diseases, which can greatly affect heart function. Surgical techniques have changed a lot over the years, motivated by the desire to achieve better results, minimize complications, and cater to a wide range of patients, including children and older adults with various health issues. These procedures can be generally divided into two main types: valve repair and valve replacement. The replacement options include both mechanical and bioprosthetic choices, along with new transcatheter technologies (Engelhardt et al., 2019).

Doctors often choose to repair the aortic valve for patients who have issues like valve insufficiency or regurgitation due to structural problems, such as prolapsed leaflets or annular dilation. This method focuses on keeping the native valve intact, which means patients won't have to rely on lifelong anticoagulation like they would with mechanical

valves. Leaflet repairs involve techniques like plication, resection of any prolapsed segments, and patch augmentation with pericardial tissue (Figure 1.3). These methods help bring things back together and enhance how the valve works (Mendoza et al., 2024). Annuloplasty is a procedure that focuses on resizing and stabilizing the valve annulus with the help of sutures or prosthetic rings. It often works hand in hand with leaflet repair to ensure the best possible outcomes (Engin and Güvenç O., 2024). The valve-sparing root replacement technique keeps the natural valve intact while replacing the affected aortic root. This approach is often used for patients with connective tissue disorders, such as Marfan syndrome (Nuche et al., 2024).

Replacement is necessary when repair just isn't an option, like in cases of severe calcific aortic stenosis or advanced aortic regurgitation with significant structural damage. Mechanical valves made from titanium and pyrolytic carbon are built to last, but they do need lifelong anticoagulation to help avoid thromboembolic complications. These are a great choice for younger patients because they are durable (Ahmed et al., 2020). Bioprosthetic valves, which are created from bovine or porcine tissue, are less likely to cause blood clots and don’t need lifelong anticoagulation treatment. However, their lifespan is limited because of structural valve deterioration, which makes them a better fit for older patients (Gao et al., 2024). In the Ross Procedure, the damaged aortic valve is replaced with the patient's own pulmonary valve, while the pulmonary valve is subsequently replaced with a cryopreserved donor valve. This approach is commonly applied in younger patients, providing opportunities for growth and great blood flow dynamics (Loshusan et al., 2024).

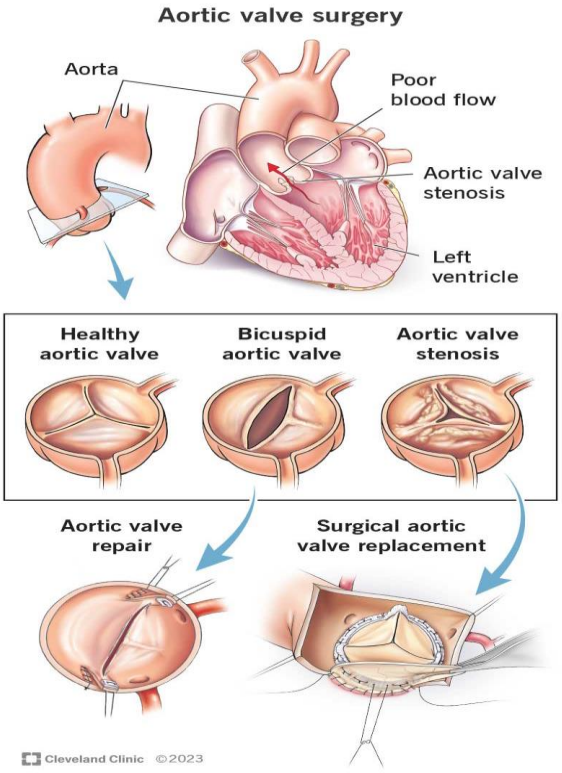

Figure 1.3 Repair and treatment options of aortic valve (Yacoub & Takkenberg, 2005)

Transcatheter Aortic Valve Replacement (TAVR) offers a less invasive option compared to open-heart surgery, mainly for patients dealing with severe aortic stenosis who face high or intermediate risks during surgery. A prosthetic valve is inserted through a catheter, typically using the femoral artery, and is placed to take the place of the damaged valve. TAVR has shown similar results to surgical aortic valve replacement (SAVR) in certain groups of patients (Figliozzi et al., 2024).

Currently, aortic valve research is ongoing in laboratories through experimental studies that utilize 3D production technologies and tissue engineering. This is due to the advancements in technology. The objective of bioengineered valve research is to develop biological valves that are capable of growth and repair by utilizing scaffolds that have been implanted with stem cells (Al-Atassi et al., 2015). 4D bioprinting innovations involve the development of valves that can adapt to physiological changes over time, thereby improving their functionality and durability (Gu et al., 2016).

1.4 Tissue Engineering as a Method for Aortic Valve Replacement

Tissue engineering is an innovative field that aims to heal or substitute damaged tissues and organs by blending biological concepts with materials science and engineering methods. Tissue engineering fundamentally revolves around three main elements: scaffolds, stem cells, and signaling molecules like growth factors. Together, these components help to establish a supportive environment that promotes tissue regeneration and functionality. Scaffolds, usually made from materials that are friendly to the body and can break down naturally, are designed to resemble the natural extracellular matrix (Sodian et al., 2000). These structures help support cells and organize their space, allowing them to adhere together, grow, and develop properly (Figure 1.4). Designing scaffolds is important because their physical properties, like porosity, stiffness, and surface chemistry, need to be customized for the specific tissue that's being regenerated. Hydrogels, polymeric meshes, and composite materials are commonly used to make scaffolds for regenerating cartilage, bone, and skin, showcasing their versatility and significance (Chen Liu X., 2017; O'Brien, 2011).

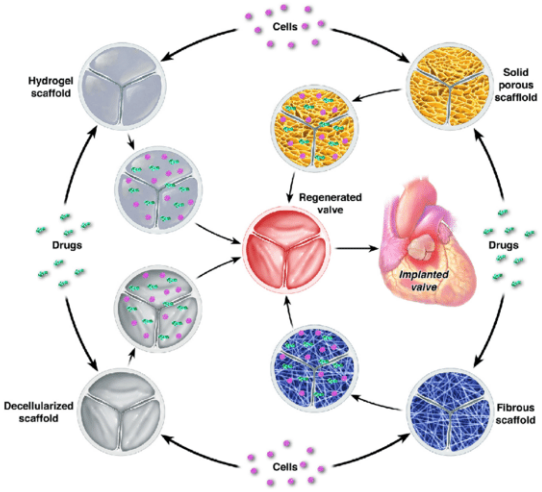

Figure 1.4 Tissue engineering approaches of heart valve replacement (Jana et al., 2014)

Stem cells are vital in tissue engineering due to their ability to self-renew and differentiate into various specialized cell types. Among these induced pluripotent stem cells (iPSCs) and embryonic stem cells (ESCs), are often used because they can create various types of tissues like osteocytes, chondrocytes, and cardiomyocytes. Stem cells have incredible

potential, not just because they can create functional tissues, but also because they can help regulate the immune response, lower inflammation, and improve blood vessel formation in damaged areas (Murphy Wang H. T. Nguyen T., 2020). For example, MSCs are good at helping bone regeneration, and iPSCs provide specific options since they originate from the patient's own cells, which helps prevent immune rejection. Using the potential of these cells has led to important progress in regenerating complex tissues such as the liver and heart, highlighting the flexibility of therapies based on stem cells (Takahashi Yamanaka S., 2006).

Signaling molecules, particularly growth factors, are essential in tissue engineering as they regulate key cellular processes such as proliferation, migration, differentiation, and ECM synthesis. Examples of these bioactive molecules include vascular endothelial growth factor (VEGF), which facilitates the formation of new blood vessels, and bone morphogenetic proteins (BMPs), which play a pivotal role in bone and cartilage regeneration. Getting these molecules delivered through scaffolds is quite a complex task. It needs careful management to make sure they are released steadily and have the desired impact (Patil et al., 2019). Recent developments in nanotechnology and controlled-release systems have made it possible to encapsulate growth factors in nanoparticles and hydrogels. This innovation helps maintain their effectiveness for a longer time while minimizing degradation (Langer Vacanti J. P., 1993). This specific regulation is especially important in tissues that need blood vessels, like muscle or skin, where VEGF plays a crucial role in creating a strong blood supply that is vital for delivering nutrients and removing waste.

Bringing these components together creates a collaborative environment that tackles the challenges of traditional transplantation methods, like the shortage of donors and issues with immune rejection. Tissue engineering has shown incredible promise in regenerative medicine, with uses that include skin grafts for burn victims, tracheal replacements, and even the creation of organs. For example, scientists have been using decellularized organ scaffolds along with stem cells and growth factors to bioengineer organs such as the bladder and trachea. These efforts have led to functional replacements that fit well into the host system (Badylak Taylor D. Uygun K., 2009). The field keeps growing with new

developments in bioprinting and organ-on-a-chip technologies, making tissue-engineered constructs even more precise and scalable.

1.4.1 Tissue engineered heart valves

Tissue-engineered heart valves (TEHVs) are an exciting development in cardiovascular medicine, providing answers to the challenges posed by traditional prosthetic valves, like the risk of blood clots, inability to grow, and concerns about how long they last (Gao et al., 2024). These tissue-engineered heart valves are designed to mimic the natural structure, function, and biomechanical characteristics of real valves (Xu et al., 2022). They combine biodegradable scaffolds, cellular elements, and bioactive substances to form living implants that can change and evolve as time goes on.

Scaffolds made from materials like polycaprolactone (PCL), polyurethane (PU), collagen, and fibrin serve as the essential building blocks for tissue development. They can be designed using methods like additive manufacturing to replicate the intricate properties of natural valves. Cells like autologous mesenchymal stem cells (MSCs), and endothelial progenitor cells are placed onto the scaffolds, helping tissue to grow while reducing the chances of immune reactions (Wells et al., 2021). Recent advances in using pluripotent stem cells allow to create valve cells that are specific to each patient, leading to better regenerative results. Also, biochemical signals like VEGF and transforming growth factor-beta (TGF-β) are added to scaffolds to enhance cell growth, differentiation, and the formation of ECM (Jana et al., 2014).

Mechanical preconditioning in bioreactors improves the biomechanical properties of tissue-engineered heart valves by subjecting them to physiological stressors, helping them to endure the hemodynamic forces found in the cardiovascular system. Innovations like 4D bioprinting, which merges 3D printing with materials that adapt to physiological changes, along with decellularized xenogeneic scaffolds filled with human cells, have really pushed the boundaries in this field. These advancements allow for the development of valves that can remodel and grow right where they are needed (Motta et al., 2021). In situ tissue engineering involves placing scaffolds directly into the patient to attract the

body's own cells. This approach shows great promise by utilizing the body's natural ability to heal, making the process simpler by cutting down on the need for extensive pre-implantation preparation (Weissman, 2000).

Even with these advancements, TEHVs still encounter challenges in ensuring reliable mechanical durability, even cell distribution, and getting the necessary regulatory approval for clinical use. Long-term studies are important to confirm their safety, durability, and effectiveness. To overcome these challenges, can be needed to keep pushing the boundaries in biomaterials, bioreactor technologies, and stem cell research. More and more, computational modeling and artificial intelligence are coming together to enhance valve design and anticipate how they perform in the body, making the creation of these next-generation implants even better (Yang et al., 2022). As research continues, TEHVs could really change the way managing heart valve diseases, especially for kids and those who need long-term solutions. They might become a key part of regenerative cardiovascular medicine in the years ahead.

1.4.2 Stem cells in tissue engineering

Stem cells are the essential building blocks of multicellular organisms, known for their ability to both self-renew and transform into different specialized cell types. These cells are crucial for development, healing tissues, and keeping everything balanced, acting as a source for replenishing cells throughout an organism's life. Their natural ability to adapt and regenerate has turned them into a key area of biomedical research, offering important insights into tissue development, disease modeling, and the exploration of new therapies. Stem cells can be generally grouped into three categories: embryonic stem cells (ESCs), adult stem cells, and induced pluripotent stem cells (Weber et al., 2015). Each type shows different levels of potency and specialized functions. Also, there are other specialized types, like totipotent and unipotent stem cells, that really broaden the range of their biological functions. Every type of stem cell plays a special role in the world of biological research and medical advancements, highlighting their unique abilities and backgrounds (Figure 1.5) (Blanpain Fuchs E., 2009).

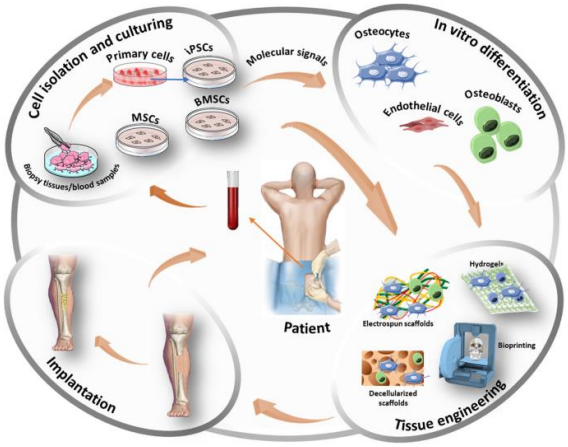

Figure 1.5 Tissue engineering paradigm from stem cells to implantation (Augustine et al., 2024)

1.4.2.1 Embryonic stem cells (ESCs)

The inner cell mass of a blastocyst, a porous structure that forms approximately 4 to 5 days after fertilization during the early phases of human embryonic development, is the source of embryonic stem cells. These cells are distinctive in that they possess the ability to differentiate into virtually any cell type within the three germ layers: ectoderm, mesoderm, and endoderm, in accordance with their pluripotent nature. Critical transcription factors, including Oct4, Sox2, and Nanog, are regulated to preserve the pluripotency of ESCs. These factors are essential in preventing differentiation, thereby maintaining the cells in their undifferentiated state. Oct4 is notably critical for the preservation of the self-renewal properties of ESCs, while Sox2 functions in conjunction with Oct4 to modulate genes that are essential for pluripotency. Nanog further fortifies this regulatory network by impeding pathways that facilitate differentiation (Thomson et al., 1998).

ESCs are indispensable for both fundamental research and clinical applications due to their capacity to remain undifferentiated while retaining the potential to develop into a variety of cell types. They are a potent model for the investigation of early human development, the comprehension of disease mechanisms, and the development of regenerative therapies that are designed to replace damaged or diseased tissues. Nevertheless, the utilization of ESCs also raises ethical concerns, as their generation necessitates the destruction of embryos, which requires careful consideration in their

regulation and application. ESCs are grown in carefully managed environments to keep their ability to become different cell types, enabling researchers to thoroughly investigate their potential for differentiation. They can create functional cells for different tissues, which have been used to study how development works, learn about genetic disorders, and investigate regenerative therapies. However, deriving ESCs means destroying embryos, which raises ethical concerns and has led to the exploration of alternative stem cell sources like iPSCs. Even though ESCs are genetically stable, there are risks of immune rejection during transplantation if the cells don't match the patients' genetics. Additionally, the risk of uncontrolled growth or teratoma formation is a major concern, which calls for strict regulation in clinical applications (Khaki et al., 2018).

1.4.2.2 Adult stem cells

Adult stem cells are multipotent cells found in various tissues throughout the body. Adult stem cells are different from ESCs because they are lineage-restricted, which means they usually differentiate into specific cell types related to the tissue they come from. For instance, hematopoietic stem cells (HSCs) found in the bone marrow can develop into all types of blood cells, whereas mesenchymal stem cells can transform into osteoblasts, chondrocytes, and adipocytes (Weissman, 2000). Adult stem cells are essential for keeping tissues balanced and helping them heal after an injury. They live in unique microenvironments or niches within tissues, where their interactions with other cells, components of the extracellular matrix, and signaling molecules help to control their activity. For example, HSCs are found in the bone marrow niche, where stromal cells and cytokines help keep them in a resting state and direct their development during blood cell formation.

On the other hand, MSCs were found in places like bone marrow, fat tissue, and umbilical cord blood, as well as a few other sources. Their ability to develop into mesodermal lineages and adjust immune responses has turned them into a key focus of research for regenerative therapies. Still, adult stem cells do have some limitations, such as their lower ability to grow and develop into different cell types when compared to embryonic stem cells. Also, as they get older, their amounts go down, and certain diseases can affect how

well they work, which creates challenges for using them in treatments (Rieder et al., 2004).

1.4.2.3 Induced pluripotent stem cells (iPSCs)

Induced pluripotent stem cells are a groundbreaking development in the field of stem cell biology. Scientists create these cells by taking regular cells, like skin or blood cells, and reprogramming them to become pluripotent (Takahashi Yamanaka S., 2006). This reprogramming brings the cells back to a state that's a lot like embryonic stem cells, enabling them to turn into almost any type of cell in the body. iPSCs have a lot in common with ESCs, such as showing pluripotency markers and being able to form teratomas when they're transplanted into mice that have weakened immune systems (Fisher et al., 2024). But iPSCs get around the ethical concerns tied to ESCs since they don't need embryos. Also, iPSCs can be specialized to individual patients, which helps lower the chances of immune rejection and supports personalized medicine. For instance, scientists have taken iPSCs from patients with genetic disorders to build disease models in the lab. This lets them explore how these diseases work and test out possible treatments.

Even though they hold a lot of potential, iPSCs come with several challenges to overcome. The reprogramming process might lead to genetic and epigenetic issues, which could affect their stability and how well they work. New developments in reprogramming techniques, like using non-integrating vectors and small molecules, are focused on addressing these challenges and improving how iPSCs can be used in clinical settings (Takahashi Yamanaka S., 2006).

1.4.2.4 Adipose-derived stem cells (ASCs)

Adipose-derived stem cells (ASCs) are isolated from adipose (fat) tissue. There are numerous similarities between these cells and bone marrow-derived MSCs in terms of their capacity to differentiate into a variety of cell lineages and self-renew. Even so, ASCs possess unique benefits, such as their abundance in adipose tissue, simplicity of harvest, and higher yield when contrasted with other stem cell sources, such as bone marrow.

Under specific circumstances, ASCs can differentiate into a diverse array of mesodermal-derived cells, including adipocytes, osteoblasts, chondrocytes, and myocytes, as well as certain ectodermal and endodermal cell types (Zuk et al., 2001). Adipose tissue, which is easily accessible through liposuction procedures or surgical fat removal, is a rich and abundant source of ASCs. A heterogeneous combination of cells, such as endothelial cells, pericytes, fibroblasts, and immune cells, is present in the stromal vascular fraction (SVF) of adipose tissue, where these cells are located. The SVF is separated after enzymatic digestion of adipose tissue, which is typically performed with collagenase. ASCs are then isolated based on their adherence to plastic culture plates in standard cell culture conditions. ASCs are a highly practicable option for regenerative medicine due to their higher yield of stem cells per gram of tissue and their greater abundance in comparison to bone marrow MSCs (Fraser Wulur I. Alfonso Z. Hedrick M. H., 2006). The potential of ASCs to facilitate angiogenesis and tissue regeneration is an asset in the therapy of chronic wounds (Gimble Katz A. J. Bunnell B. A., 2007). ASCs are currently being investigated for a variety of clinical applications. ASCs are involved in the restoration of bone and cartilage in orthopedic conditions such as osteoarthritis and fractures. Moreover, they contribute to the regeneration of myocardium and the restoration of vascular tissue by secreting angiogenic factors and transforming into vascular cells. In addition, researchers found that ASCs have the capacity to transdifferentiate into non-mesodermal lineages, including neuronal-like cells, hepatocytes, and pancreatic β-cells, under specific culture conditions. This underscores their potential for a variety of regenerative therapies (Mizuno, 2009).

1.4.3 Heart valve tissue engineering scaffolds

Scaffolds play a crucial role in heart valve tissue engineering by offering a three-dimensional structure that helps cells adhere, proliferate, develop, and create the extracellular matrix. These structures need to mimic the biochemical environment of heart valves, all while being tough enough to manage the changing forces of the cardiovascular system. There are two main types of scaffolds that are commonly studied in this area: (i) Decellularized natural heart valve scaffolds derived from allogenic or xenogeneic sources, and (ii) fully synthetic scaffolds fabricated from a combination of synthetic and

natural polymers. Both approaches come with their own set of pros and cons, and researchers are actively looking into them to understand the challenges of heart valve tissue engineering.

Acellular natural heart valve scaffolds, which come from either allogenic (human) or xenogeneic (animal) sources, make use of the natural structure and composition found in native extracellular matrix. The decellularization process takes away the cellular parts from donor tissues but keeps the complex structure of the extracellular matrix, along with its strength and important signaling molecules like glycosaminoglycan, elastin, and collagen (Petreaca & Martins-Green, 2020). These scaffolds replicate the unique mechanical properties of natural heart valves, which are crucial for their proper function. Allogenic scaffolds are ideal because they work well with the human body and lower the chances of immune rejection. However, the limited availability of human donor tissues holds back their broader use. Xenogeneic scaffolds, typically derived from porcine or bovine valves, are more readily available but pose risks of immunogenicity and potential zoonotic disease transmission. Researchers have come up with various decellularization techniques, like enzymatic, chemical, and physical methods, to address these risks while keeping the essential structural and functional qualities of the ECM (Rieder et al., 2004). These scaffolds show great compatibility with the body and assist in the recellularization process using cells from patients, making them a good fit for personalized regenerative treatments. Still, it's tough to get consistent decellularization while keeping the ECM intact, and researchers also must deal with the risk of calcification in living organisms.

Totally artificial scaffolds created from synthetic and natural polymers offer a much more flexible choice than natural scaffolds (Figure 1.6). Synthetic polymers such as polycaprolactone, polyurethan, polylactic acid are favored for their customizable mechanical properties, reliable stability, and straightforward processing. There are ways to work with these materials, such as using electrospinning and 3D printing techniques. This enables the development of scaffolds with particular shapes and pore structures, crafted to mimic the natural function of a heart valve (Dasi Ge L. Sotiropoulos F. Yoganathan A. P., 2009). Also, synthetic polymers can be created to break down at certain rates, which helps match the timing of tissue healing. Even so, synthetic scaffolds

typically lack bioactivity by themselves and require enhancement with peptides, growth factors, or elements from the extracellular matrix to support proper cell adhesion and integration. Researchers have produced hybrid scaffolds that mix synthetic and natural polymers to get around this limitation (Ehrlich, 2019). Natural polymers such as collagen, alginate and gelatin form surfaces that facilitate cell interactions, whereas synthetic polymers contribute to strength and durability. Bringing together natural polymers and synthetic scaffolds creates hybrid materials that blend the best features of both (Hanna et al., 2010). Collagen-PCL composites have shown that they can support strong cell adhesion and growth, all while maintaining the important mechanical properties needed for valve function (Chen Liu X., 2017). Additionally, bio-fabrication technologies, like 3D bioprinting, have made it possible to create scaffolds for individual patients. These scaffolds incorporate growth factors such as VEGF and TGF-B to enhance the formation of new blood vessels and support cellular differentiation. Being able to create scaffolds that have carefully controlled mechanical and biological features marks a significant advancement in this field. Still, there are challenges to overcome, such as achieving lasting mechanical stability, avoiding immune reactions, and ensuring even distribution of cells and extracellular matrix deposition.

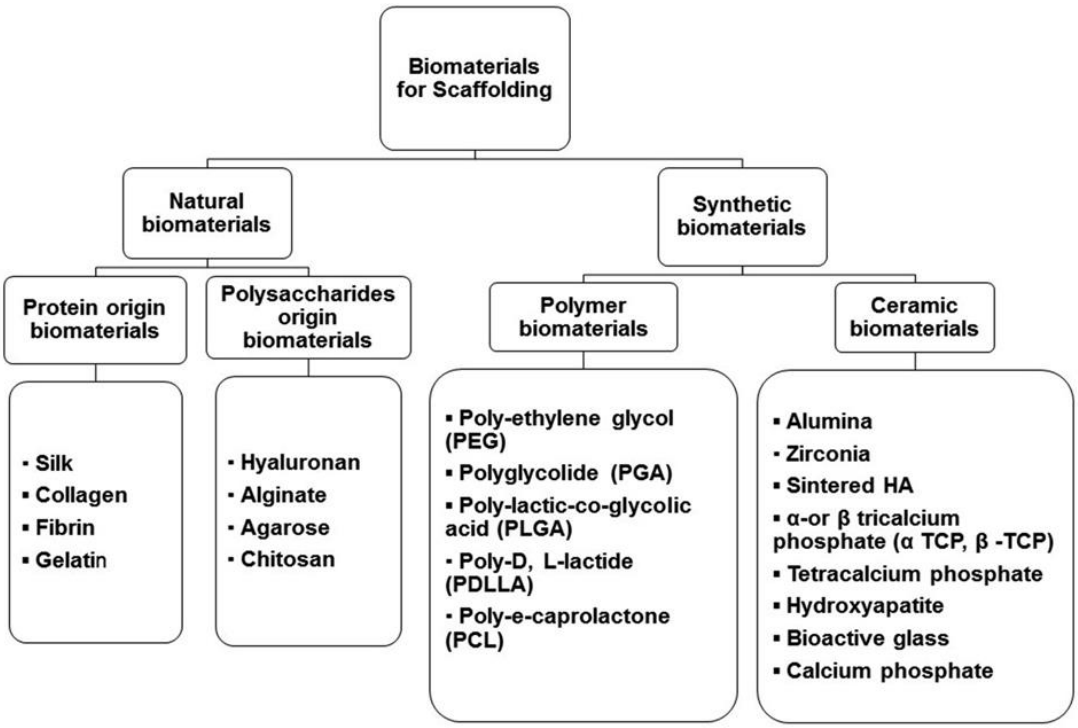

Figure 1.6 Biomaterials for scaffolds (Alaribe et al., 2016)

1.4.4 Scaffold manufacturing methods

In tissue engineering, the methods used to create scaffolds are crucial for building structures that resemble the extracellular matrix. Among these, spinning techniques, 3D printing, and 3D bioprinting have come up as creative ways to make scaffolds designed for tissue engineering needs. Every method brings its own set of advantages, challenges, and uses, playing a key role in the progress of regenerative medicine.

1.4.4.1 Spinning techniques

Spinning techniques, especially electrospinning, are well-known for their capability to create nanofibrous scaffolds that mimic the ECM. Electrospinning uses a high-voltage electric field to stretch a polymer solution into very fine fibers, which are then gathered into nonwoven mats (Bhattarai et al., 2005). These mats have a large surface area compared to their volume, which is important for cells to adhere, expand, and get the nutrients they need (Greiner & Wendorff, 2007). Electrospun scaffolds are made from various polymers, such as synthetic ones like poly (lactic-co-glycolic acid) (PLGA) and natural materials like collagen or gelatin. This allows for careful management of mechanical properties, degradation rates, and how well they work with biological systems (Zhang et al., 2005). Advanced methods, like coaxial electrospinning, enable the production of core-shell fibers that can deliver bioactive agents such as growth factors or medications, which helps improve tissue regeneration (Huang et al., 2003).

There are other spinning methods like wet spinning and melt spinning that come with their own set of benefits. Wet spinning is a process where polymer solutions are injected into coagulation baths, resulting in aligned fibers that are great for uses like tendon and ligament scaffolds. Melt spinning skips the use of harmful solvents by using heat to pull fibers, which makes it a more sustainable choice for biomedical applications (Teo & Ramakrishna, 2006). Although these methods are not as widely used as electrospinning, they offer important alternatives for scaffolds that need mechanical properties.

1.4.4.2 3D printing techniques

3D printing, often called additive manufacturing, has really changed the rules for making scaffolds. It allows to create structures with unique shapes and exact designs that fit the needs perfectly (Figure 1.7). This method of building things layer by layer, using computer-aided design (CAD) models, gives the ability to control how porous the scaffold is, its mechanical properties, and what materials to use. This control is crucial for mimicking the intricate structures of tissues (Ovcharenko et al., 2014).

Fused deposition modeling, or FDM, is a popular way to create 3D printed scaffolds. FDM is all about extruding thermoplastic polymers like polycaprolactone or polylactic acid through a heated nozzle. This method is affordable, can be scaled up easily, and works great for applications that need to support weight, like bone and cartilage tissue engineering (Saidy et al., 2019). Still, its resolution is not as high as some other 3D printing methods, which could restrict its use for creating detailed tissue structures (Hockaday et al., 2012).

Stereolithography (SLA) uses a special resin that hardens when exposed to a laser or light, allowing it to build up layers of material one at a time. SLA provides excellent resolution and smooth surface finishes, which makes it perfect for crafting scaffolds with intricate microarchitectures. Techniques such as digital light processing (DLP) enhance speed without sacrificing precision, which makes them great for creating scaffolds for soft tissues like skin and cartilage (Yadid et al., 2022).

Selective laser sintering (SLS) uses powdered materials then a laser fuses these materials together, creating scaffolds that offer great mechanical strength and intricate shapes. This method works well with various materials, like polymers and ceramics, which makes it useful for engineering bone and dental tissues (Schiele et al., 2010). However, SLS faces challenges due to the limited availability of biocompatible and biodegradable powders, and it might need post-processing to get rid of residual components (Wu et al., 2019).

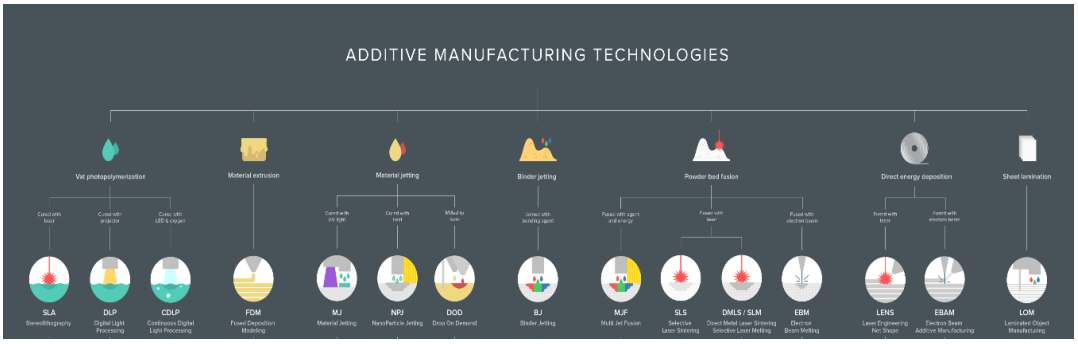

Figure 1.7 Additive manufacturing methods (Varghese et al., 2022)

1.4.4.3 3D bioprinting techniques

3D bioprinting is a sophisticated scaffold construction method that incorporates living cells, bioactive compounds, and biomaterials into three-dimensional structures. This technique provides exceptional capability for generating functional tissue constructions by the careful arrangement of cells and extracellular matrix-like components (Murphy & Atala, 2014).

Extrusion-based bioprinting is the predominant 3D bioprinting method, which entails the deposition of bioink—a combination of cells and hydrogels—via a nozzle to construct three-dimensional objects. This technique facilitates the production of large-scale structures with intricate geometries, including vascularized tissues and cartilage. However, it frequently compromises resolution for speed, which may restrict its capacity to reproduce intricate anatomical details (Gudapati et al., 2016).

Inkjet bioprinting uses droplets of bioink that are sprayed onto a surface to build detailed structures. Applications needing accurate cell patterning, like vascular and brain tissues, are a good fit for this method. But there's a downside: the viscosity of bioinks can be a problem. If the materials are too thick, they might block the printing nozzles (Bajaj et al., 2014).

Laser-assisted bioprinting (LAB) involves using laser to place bioink drops onto a surface. LAB offers great precision and works well for placing cells and biomaterials in tiny, detailed setups. This technique shows great potential for creating complex tissues

like skin and neural tissues, but it's still too expensive for it to be widely used (Schiele et al., 2010).

Stereolithography-based bioprinting brings together SLA technology and biocompatible hydrogels, making it possible to create detailed tissue structures. This method is great at building complex vascular networks and microarchitectures, all while keeping the cells alive (Murphy Wang H. T. Nguyen T., 2020). Even with these benefits, its use is restricted by the lack of suitable photopolymerizable bioinks.

1.4.5 Signaling molecules and their role in tissue engineering

Signaling molecules are essential in tissue engineering as they regulate cellular behaviors such as growth, differentiation, migration, and extracellular matrix production. Growth factors are part of larger polypeptide molecules that are naturally released by healthy cells in the body. Research has shown that GFs react in many ways depending on the concentration levels and how long they are exposed to the cells. VEGF and TGF-β1 are two key factors that have been closely examined for their significant roles in enhancing the growth of new blood vessels, healing tissues, and supporting regeneration (Murphy Wang H. T. Nguyen T., 2020).

VEGF is a powerful signaling protein that is crucial for vascularization and the process of creating new ones, known as angiogenesis. VEGF-A stands out as the most researched because it is important for the growth, movement, and survival of endothelial cells (EC) (Ferrara et al., 2003). VEGF attaches to its receptors which are found on the surface of endothelial cells. The interaction between VEGF and VEGFR triggers signaling pathways that are important for cells. This includes the PI3K/Akt pathway, which helps cells survive, and the MAPK/ERK pathway, which participates in cell growth and movement. These pathways work together to improve how endothelial cells function, allowing them to create structures like capillaries (Ferrara et al., 2003). VEGF plays a pivotal role in tissue engineering, especially in situations where forming blood vessels is essential, like in bone, skin, and heart tissue engineering. Adding VEGF to scaffolds or delivery systems helps create blood vessels in engineered tissues, which is crucial for providing oxygen

and nutrients to cells while also aiding in waste removal. For instance, hydrogels loaded with VEGF have been found to boost the formation of new blood vessels in tissues that lack oxygen and to help wounds heal better (Richardson et al., 2001). Delivering VEGF in tissue engineering comes with its own set of challenges, mainly because it has a short half-life and breaks down quickly in the body. Researchers produce controlled release systems like using nanoparticles for encapsulation or embedding in hydrogels to make sure that substances are released steadily and delivered right where they are needed. These methods help lower the chances of unintended effects and enhance treatment results (Engler, 1996).

TGF-β plays a role in many cellular activities, such as differentiation, proliferation, apoptosis, and the synthesis of the ECM. It is part of the TGF-β superfamily, which also has TGF-β2 and TGF-β3 in it. TGF-β1 plays a crucial role in managing fibrosis, immune responses, and how tissues are remodeled (Massagué, 2012). TGF-β1 works by attaching to TGF-β receptors (TGF-βR I and II) found on the cell surface, which starts a series of signaling events inside the cell. This process brings in Smad proteins (Smad2/3), which move into the nucleus to help control the transcription of genes that play a role in ECM production and cell differentiation. Other pathways like MAPK and PI3K play a role in the various effects of TGF-β1 as well (Hinck et al., 2016; Massagué, 2012). TGF-β1 plays a crucial role in the production and remodeling of the extracellular matrix, which is vital for creating tissues like cartilage, bone, and skin. It helps mesenchymal stem cells turn into chondrocytes and osteoblasts, which supports the regeneration of cartilage and bone. TGF-β1 promotes fibroblasts to create collagen and other ECM proteins, which helps improve wound healing and tissue (Hinck et al., 2016). Just like VEGF, TGF-β1 needs to be delivered carefully to get the right therapeutic results without causing any negative effects. Controlled release systems like polymeric scaffolds or microspheres are used to deliver TGF-β1 in a way that is both sustained and localized. These systems work well for repairing cartilage, as TGF-β1 gradients can guide chondrocyte differentiation and help produce the matrix (Richardson et al., 2001).

1.4.6 Controlled drug-delivery systems in tissue engineering

To overcome the limitations associated with conventional drug administration methods—like varying therapeutic levels, rapid drug clearance, and unwanted side effects—researchers have created controlled drug delivery systems (CDDS) in tissue engineering. In the mid-20th century, progress in polymer science and the development of early sustained-release technologies sparked interest in researching these systems. The basis for today's delivery technologies was laid by the initial methods of drug release regulation, such as matrix and reservoir-based systems (LANGER & FOLKMAN, 1976). Biodegradable polymers like poly (lactic-co-glycolic acid) changed the methods in the 1980s. They made it possible to deliver drugs right where they're needed, with a controlled breakdown and less impact on the rest of the body. Over time, the combination of nanotechnology, biomaterials, and biological engineering has really pushed CDDS into important areas like tissue engineering, and personalized therapeutics(Lanuti et al., 2016).

Controlled drug delivery systems are crucial in tissue engineering because of the complex demands for precise timing and location of biological signals that are crucial for tissue regeneration. Traditional ways of delivering drugs often struggle to keep the right levels of active ingredients in the body, which can result in less effective treatments. CDDS overcome these challenges by providing bioactive molecules like growth factors and cytokines in a way that's both localized and sustained (Heidari et al., 2015). This ability is especially important for tissue regeneration processes, like angiogenesis and ECM deposition, where molecules such as VEGF and TGF-β1 must be released at the right times and places (Massagué, 2012). Recent developments in hydrogels, nanoparticles, and 3D-printed scaffolds have made it possible to finely tune how drugs are released, which enhances the effectiveness of engineered tissues and constructs.

Some important aspects of CDDS in tissue engineering are their capacity to deliver drugs steadily and right where they're needed, preserve bioactive molecules from breaking down, and minimize side effects throughout the body. Today's systems use smart materials that react to changes in the environment, like pH or temperature, allowing for the release of drugs when needed (Bajaj et al., 2014). Also, new developments in nanotechnology and bioconjugation have made it possible to deliver several bioactive

agents together, creating synergistic effects that improve tissue repair and regeneration. These features make CDDS essential in tissue engineering, allowing for careful control over how therapeutic agents are delivered and playing a key role in creating bioengineered tissues that closely resemble the complexity of natural tissues. As the field keeps growing, CDDS are set to take on increasing significance in pushing forward regenerative medicine and personalized therapies.

1.5 Scope and Novelty of the Thesis

The aim is to use the production of aortic valves that are personalized, live, functional, and have the potential to eliminate problems encountered in current clinical applications by producing a unit model of the aortic valve structure with 3D bioprinting and biomimetic culture. The research question of the proposed thesis is that it is possible to provide geometric production of the biomimetic aortic valve structure with 3D modeling, to produce a mesenchymal stem cell-derived aortic valve equivalent with a complex 3D bioprinting approach, and to observe its physiological properties in vitro to produce the functional production of this structure ready for potential clinical application. With this approach, it is aimed to establish a basis for animal experiments and subsequent clinical studies to be carried out in future projects by carrying out preclinical studies on the production of autologous functional aortic valve equivalents in a laboratory environment. In testing the proposed approach, preliminary research and examinations required for autologous production specific to pediatric patients using 3D bioprinted personalized aortic valves together with mesenchymal stem cells will be carried out within the scope of the thesis. In this context, in the 3D production of aortic valve unit models modeled in accordance with the anatomical structure, polyurethane was preferred for the flexibility of the structure and its long-term effectiveness, and GelMA (Gelatin Methacrylate) hydrogel, which provides an environment suitable for differentiation and proliferation for cells and also provides stability thanks to cross-linking with UV light, was preferred, and this dual structure was cultured in an in vitro environment by producing a 2-phase cell scaffold with growth factors and cells. The importance of this study is that it provides both a functional and cost-effective approach because of the in vitro production of heart valve equivalents in the desired dimensions needed in the clinic and their cultivation using a single cell source.

2. MATERIALS & METHODS

2.1 Materials

The materials employed in this thesis, their purposes and companies are given in Table 2.1.

Table 2.1 Materials employed in this study

Material	Brand/Company	Use
Capsule Production		
Poly(caprolactone) (PCL) oligomeric form (M_w=37000 g/mol)	Perstorp AB	Particle Preparation
Polyvinyl alcohol (PVA)	Sigma Aldrich	Particle Preparation
Dichloromethane (DCM)	Sigma-Aldrich	Particle Preparation
Bovine Serum Albumin (BSA)	Sigma-Aldrich	Model protein
Recombinant Human TGF-B1	Biolegend	Growth factor
Recombinant Human Vascular Endothelial Growth Factor-165	Biolegend	Growth factor
Trizma® base	Merck	Buffer
Hydrochloric acid (HCL)	Sigma-Aldrich	Buffer
Dulbecco's Phosphate Buffer Saline (PBS)	Sigma-Aldrich	Buffer

Table 2.1 Materials employed in this study (continued)

Material	Brand/Company	Use
Scaffold Production		
Thermoplastic Polyurethane Ultrafuse 85A	BASF	Polymer
Gelatin (porcine skin, type A)	Sigma Aldrich	GELMA-Synthesis
Methacrylic Anhydride	Sigma-Aldrich	GELMA-Synthesis
SnakeSkin dialysis membrane	ThermoFisher	GELMA-Synthesis
Tetrahydrofuran	Emplura	Solvent
Lithium Phenyl (2,4,6- trimethylbenzoyl) phosphinate	Sigma-Aldrich	GELMA-Crosslink

Material	Brand/Company	Use
In Vitro Study		
Adipose-derived stem cells (ASCs)	Isolated from human abdominal fat tissue	*In vitro* studies
Fibroblast growth factor (bFGF)	Sigma-Aldrich	ASC expansion medium
High-glucose DMEM	Biological Ind.	ASC expansion medium
Fetal Bovine Serum (FBS)	Biological Ind.	ASC expansion & differentiation medium
Penicillin-Streptomycin (10X) Solution	Biological Ind.	ASC expansion & differentiation medium
Trypsin	Biological Ind.	Cell passaging

Table 2.1 Materials employed in this study (continued)

Material	Brand/Company	Use
Assays		
Alamar Blue	ThermoFisher	Cell viability analysis
Alexa Fluor 488 Phalloidin, DAPI	ThermoFisher	Morphologic study
Bovine Serum Albumin (BSA)	Sigma-Aldrich	Immunofluorescent staining
Mouse Monoclonal Anti-CD31 antibody	Abcam	Vascularization analysis
ELISA Testing Assays for VEGF and TGF-B1	Elabscience	Release Kinetic Analysis
Triton X100	Merck	Cell permeabilization
Tween20	Merck	Cell permeabilization
Paraformaldehyde	Merck	Cell fixation

2.2 Methods

2.2.1 Encapsulation of growth factors and release study

The methodology established in other investigations was followed in the manufacture technique for PCL capsule fabrication (Yilgor et al., 2009). Capsules were manufactured using the double-emulsion technique. PCL was dissolved in methylene chloride and infused with TGF-B1/VEGF separately, followed by sonication for 60 seconds at a frequency of 50 Hz (Bandelin electronic GmbH & Co. KG, Germany). %10 (w/v) of PCL were employed to produce to capsules according to previous study has made before (Goker et al., 2024). This emulsion was subsequently incorporated into a 4% (w/v) polyvinyl alcohol (PVA) solution, and sonication was conducted once more under the same conditions. A 0.3% (w/v) PVA solution was used to homogenize the double

emulsion, and the solvents were subsequently evaporated. The capsules were rinsed with Tris-HCl (10 mM, pH 7.5) and lyophilized for 24 hours (Figure 2.1).

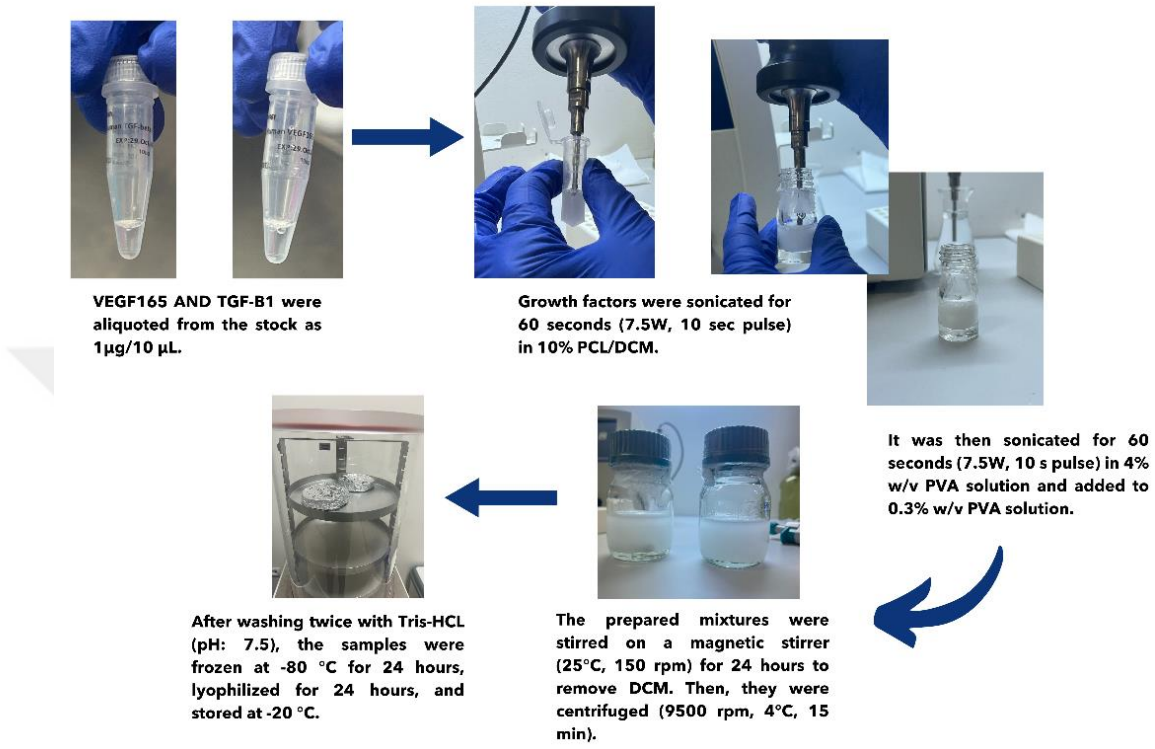

Figure 2.1 Growth Factor encapsulation process

Growth factor release was quantified using enzyme-linked immunosorbent assay (ELISA). Samples were collected from conditioned media or biological fluids at different timestamps and stored at -80°C until. Specific ELISA kits for the target growth factors, were obtained from (Elabscience, China), and assays were performed according to the protocol. First, 100 µL of each standard or sample which are collected at different timestamps (1, 2, 4, 6, 10, 14 and 21 days) was added to pre-coated 96-well plates and incubated at 37ºC. Wells were then washed with the supplied buffer, and the appropriate enzyme-conjugated secondary antibody was added, followed by incubation and additional washes. Absorbance at 450 nm was measured using a microplate reader, and growth factor concentrations were determined using a standard curve constructed from known concentrations of the target growth factor. All samples were run in duplicate or

triplicate to ensure reproducibility, and data were analyzed to assess the release profile and response to experimental conditions.

2.2.2 Scanning electron microscopy (SEM) imaging

Scaffolds and prepared capsules were examined by SEM imaging to observe cell behavior and morphology. For this purpose, samples fixed with 3.7% (w/v) PFA were washed using PIPES buffer and kept at -80ºC overnight, then lyophilized and dried. Then, surfaces were coated with gold and analyzed using QUANTA 400F Field Emission Scanning Electron Microscopy in METU central laboratory.

2.2.3 Design of aortic valve unit scaffolds

Designing aortic valve unit scaffolds for tissue engineering requires a thoughtful approach to mimic the complex structure, mechanics, and functions of natural valves. When designing scaffolds, it's important to replicate how natural aortic valves behave mechanically. These valves are stronger and stiffer around their circumference compared to their radial direction, allowing them to handle pressures between 10 and 80 mmHg and endure up to 40 million cycles each year (Hasan et al., 2014). This variation helps the valve leaflets fit together properly and keeps blood flow regulated in an effective manner. Also, using biofunctionalization strategies, like incorporating growth factors such as VEGF and TGF-β1, promotes endothelialization, ECM synthesis, and cellular differentiation, which boosts the scaffold's ability to regenerate (Richardson et al., 2001). The scaffold here was designed to be produced simultaneously with an ink obtained by dissolving polyurethane, a synthetic polymer, in tetrahydrofuran (THF), and a bioink developed with GelMA/Gelatin, ASCs and growth factors. It is planned to mimic the anatomical, anisotropic, durable and flexible structure of the unit model of the aortic valve with the designed scaffold (Figure 2.2).

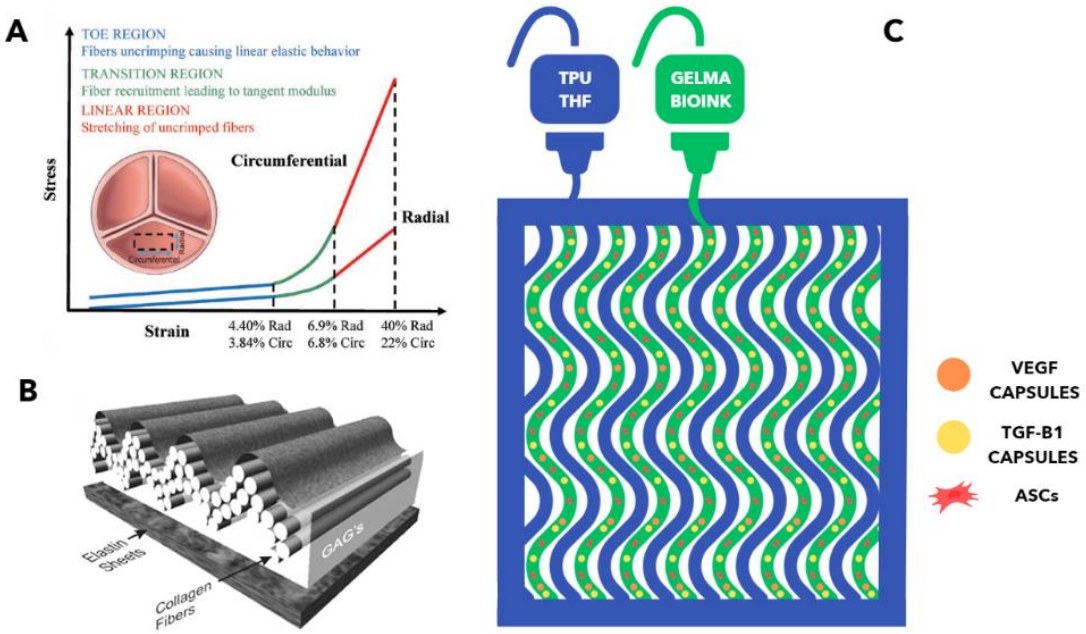

Figure 2.2 Design and properties of aortic valve scaffold (a) stress distribution on heart valve according to directions (b) arrangement of collagen fibers (c) manufactured scaffold inner pattern (Saidy et al., 2019)

2.2.4 Preparation of inks for 3D printing

2.2.4.1 Preparation of GelMA/Gelatin bioink

GelMA hydrogels, which form covalent cross-links when exposed to UV light in the presence of a photo initiator, have garnered significant attention in biomedical applications (Li et al., 2019). Recent research highlights their potential as promising materials for bioprinting, enabling the fabrication of complex 3D structures through photopolymerization and additive manufacturing techniques utilizing UV light (Zhu and Yang L., 2024). Studies suggest that low-concentration GelMA hydrogels (≤5 w/v %) are particularly suitable for bioinks containing cells due to their ability to support enhanced cell growth (Colosi et al., 2016). However, low-concentration GelMA bioinks present notable challenges during extrusion-based 3D printing. First, their lower viscosity can result in instability during extrusion, leading to uneven structures. Second, the slow gelation rate of these hydrogels during the transition from liquid to solid complicates maintaining structural integrity and sensitivity post-printing. Third, their gel phase lacks

sufficient mechanical strength to preserve the scaffold's intended shape. On the other hand, while high-concentration GelMA bioinks (over 15 w/v %) provide better printability, their excessive GelMA content can negatively impact cell viability and migration within the bioink (Zaimi et al., 2024). The primary challenge in utilizing GelMA hydrogels for tissue engineering scaffolds lies in achieving an optimal balance between printability and biological functionality.

This thesis explores how blending GelMA with gelatin can improve the processability of low-concentration GelMA bioinks. Gelatin, which comes from collagen, is highly effective at helping cells adhere and spread out because it has special sites which promote cell adhesion. Also, gelatin is less likely to cause an immune response and dissolves more easily than collagen (Gu et al., 2016). Adding gelatin helps control the thickness of GelMA bioinks and also introduces a reversible thermo-crosslinking method alongside the irreversible photo-crosslinking of GelMA (Schumacher et al., 2018). The two-step crosslinking process helps make it easier to work with low-concentration GelMA/gelatin bioinks. The GelMA/gelatin bioink was prepared by reviewing the literature within the project's scope, and the final concentration was determined through printing optimizations.

In this process, porcine skin gelatin (Sigma, porcine skin gelatin, type A) was taken, and a solution was prepared and mixed with a concentration of 10% w/v using Carbonate-Bicarbonate Buffer. 0.1 ml/gram-gelatin methacrylic anhydride was added dropwise to the solution at a rate of 0.5 ml/min until the target volume was reached. The pH was checked every hour during the 3-hour reaction and adjusted to 9. At the end of 3 hours, the pH was adjusted to 7.4 and the reaction was stopped. To purify the methacrylated gelatin, the reaction mixture was subjected to a dialysis process. During this process, the product was placed inside a suitable dialysis membrane (SnakeSkin, 10 K MWCO, ThermoFisher) in distilled water and purified by changing the dialysis water daily for 3 days. Thus, the reaction products and excess methacrylic anhydride were removed. When the dialysis process was completed, the product was dried by lyophilization for 5 days. The resulting GelMAs were weighed and stored at -20 degrees. The synthesis steps are shown in Figure 2.3.

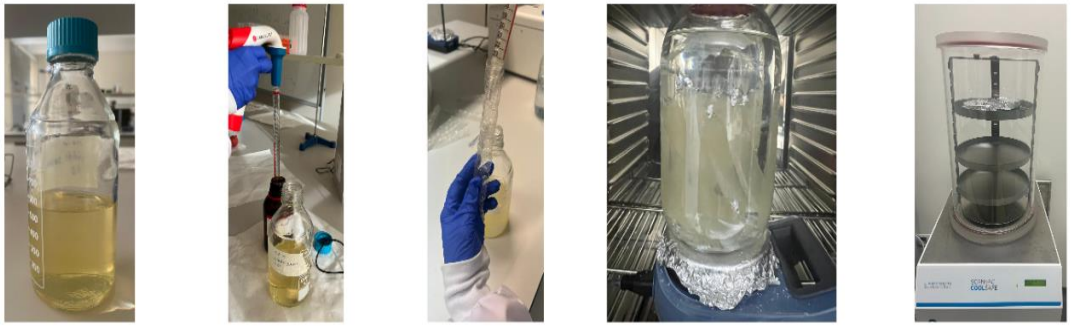

Figure 2.3 GelMA synthesis procedure

To determine the most suitable parameters for both cell viability and printability of GelMA/Gelatin concentration to be used in the project, literature was reviewed, and 3D printing trials were taken at different ratios. GelMA and gelatin synthesized with the method described above were used for all solutions and kept in PBS at 37°C for 1 hour and a homogeneous mixture was obtained. Then, it was kept at room temperature and printing was started when it reached 25°C. 0.5% (w/v) lithium-phenyl-2,4,6-trimethylbenzoylphosphinate (LAP) was added to each material to provide photo-crosslinking and crosslinking was done for 40 seconds from 15 cm with a 365 nm UV light source (Figure 2.4).

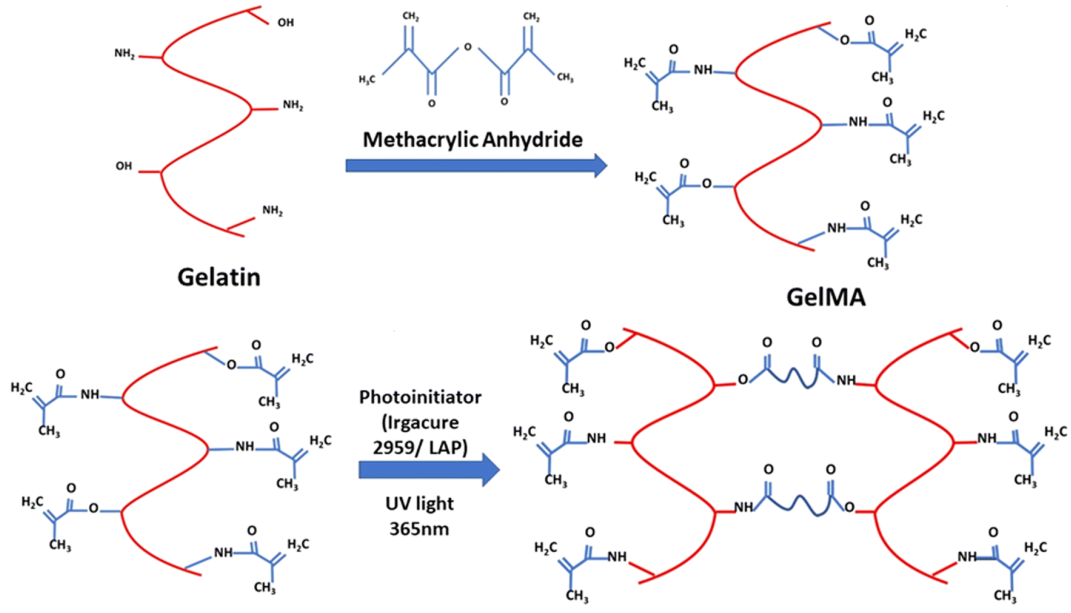

Figure 2.4 GelMA synthesis and cross-linking (Ghosh et al., 2023)

2.2.4.2 Preparation of TPU ink

TPU ink is a type of ink prepared using polyurethane and THF based solvents, customized for biomaterial and cellular applications. TPU has become an important material in applications such as tissue engineering and implants thanks to its flexible structure. THF is an organic solvent that increases the solubility of TPU thanks to its low boiling point and excellent dissolving capacity. These properties of TPU and THF are combined in the ink formulation and provide an ideal structure for scaffold applications. This mixture is specifically employed in scaffold production, providing a supportive framework for cell growth, proliferation, and structural organization. While the mechanical properties of TPU allow for the creation of flexible and durable structures, its properties compatible with biological systems minimize cellular toxicity. The compatibility of THF with TPU helps control the viscosity of the ink and ensure stable flow from the printer nozzle. The importance of this ink in scaffold applications comes from the customizable structure of this ink. TPU ink shows superior performance in scaffold structures that require both mechanical strength and biocompatibility, especially in the imitation of soft tissues and organ-like structures. BASF Ultrafuse TPU 85A was used as polyurethane in the project. The polyurethane material was used by dissolving it in tetrahydrofuran (Emplura, 99% Purity). In order to determine the solution concentration, different %w/v TPUs were added to THF and left to stir for 1 hour at 50°C and then for 24 hours with the temperature off in a magnetic stirrer. Concentration optimization was performed, and printing parameters were determined.

2.2.5 Mechanical testing

The mechanical properties of the different designed scaffolds were tested in a mechanical testing machine (Shimadzu Autograph AGS-X Series, Japan) at a conditioned environment of ~47% moisture balance and 20 °C temperature. In this test, tensile dumbbells produced with a 3D printer in accordance with DIN ISO 527-2-5A standard were used for pure TPU, and the test was applied with a 5 kN load cell at 20 mm/min (Figure 2.5). ASTM D3822 standard was used to measure the mechanical strength of the TPU/THF solution. After THF evaporation (1 hour), the samples were cut into 10 mm x

50 mm rectangular pieces, and the test was applied with a 5 kN load cell at 5 mm/min. Percentage elongation, maximum tensile strength and young modulus were calculated from the tests (n=5).

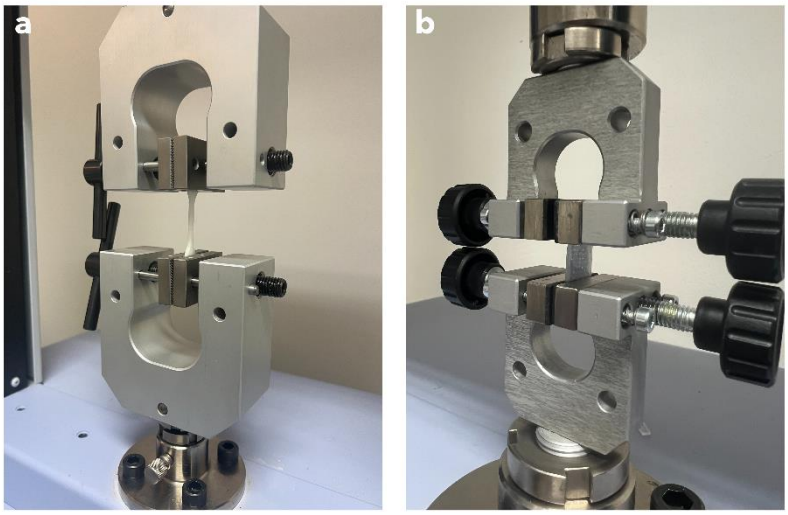

Figure 2.5 Mechanical Testing Procedure (a) 3D-printed TPU dumbbell (b) manufactured scaffold with GelMA

2.2.6 Cytotoxicity test

The initial step was to conduct an indirect cytotoxicity test to determine the biocompatibility of the scaffolds that were produced, specifically whether they released extracts that could be biologically hazardous. The polymers' biocompatibility was assessed using the MEM-extraction test, as outlined in ISO 10993/EN 30993. The four groups that were employed in the experiment were as follows: TPU1 (sample expected to be tested 1 minute after printing), TPU60 (sample expected to be tested 60 minutes after printing), positive control, and negative control (latex). The sterile falcon tubes were used for setting the samples, which were shaped into 1 cm x 1 cm diameters. TPU samples were sterilely manufactured and immediately inserted into the culture medium. The extraction fluid was composed of standard cell culture medium. The medium's composition is as follows: 10% FBS and 1% penicillin/streptomycin in high-glucose DMEM. The samples were kept in a 10 mL extraction solution at 37°C and subjected to continuous stirring at 60 rpm for 24 hours. The extraction liquid was collected into sterile 15 mL falcons after passing through a 0.2 µm membrane filter at a duration of 24 hours.

The L929 mouse fibroblast cell line was employed in the cytotoxicity assay. L929 cells from passage 20 were thawed and transplanted to T75 flasks in a standard cell culture medium. Afterward, the cells were detached from the flask using trypsin and seeded into 24-well cell culture plates at a concentration of 10,000 cells/cm² (20,000 cells for the 24-well plate) with three replicates for each group. The cells were cultured in incubator at 37°C, 5% CO2 for 24 hours. The extraction fluids were added to the cell layers at a concentration of 500 µL/well after the cells had been cultured under standard conditions for 24 hours and reached approximately 70% confluence. Morphological evaluations were conducted using a microscope. After the addition of the extraction fluids, the cell layer's spread (confluency), the quantity of the dead cells, and changes in cell morphology were assessed through microscopic examination at 24, 48, and 72 hours. The Alamar Blue® (US Biological) method was employed to determine the number of viable cells in the wells at a duration of 72 hours. A colorless DMEM solution containing 5% Alamar blue agent was added and incubated in the dark at 37°C and 5% CO2 for 1 hour. At the end of the hour, 200 µL of the test sample was extracted from each sample three times and transferred to a 96-well microplate. Table 2.2 outlines the evaluation criteria used to analyze data obtained from microscopic examination and cell counting. The data were adjusted relative to the negative control group and scored accordingly. An average score was calculated based on the first three criteria: cell layer distribution, number of dead cells, and changes in cell morphology. This average was subsequently combined with the score from the final criterion, cell growth inhibition, to calculate the overall cytotoxic response index, which ranges from 0 to 8. (Table 2.3).

Table 2.2 Evaluation criteria of cytotoxicity test

Analys	Evaluation Criteria	Grade
Cell confluency	%100	0
	%90-100	1
	%60-90	2
	%30-60	3
	%0-30	4
Dead cell (floating cell)	%0	0
	%0-5	1
	%5-10	2
	%10-20	3
	>%20	4
Change in cell morphology	no	0
	low	1
	moderate	2
	high	3
	very high	4
Cell growth inhibition	%0-10	0
	%10-30	1
	%30-50	2
	%50-70	3
	%70-100	4

Table 2.3 Cytotoxic response index value

Cytotoxic response note	Reactivity	"Material is cytotoxic"
0-1	No	No
1-3	Low	No
3-5	Moderate	Reevaluate
5-7	High	Yes
7-8	Very High	Yes

2.2.7 3D bioprinting of scaffolds

Steps of cell isolation and characterization were omitted, and ASCs previously isolated in a study by (Ergene et al., 2019) were utilized for all cell culture experiments in this study. To culture the required number of ASCs (Passage 2), T-75 tissue culture flasks were employed with a standard growth medium. The cells were maintained in a stem cell expansion medium consisting of high-glucose DMEM, supplemented with 10% FBS, 1% Penicillin/Streptomycin (P/S), and 1 ng/mL FGF-2, under conditions of 37°C and 5% CO_2. Once the cells reached 70% confluence, they were detached using trypsin and transferred to T-175 flasks for further expansion. Following another round of 70% confluence, the cells were quantified using trypan blue (Biochrom, UK) and a hemocytometer. Customized 3D models were fabricated using a 3D bioprinter (Envisiontec GmbH, Germany) equipped with dual print heads in a cabinet which is sterilized by germicidal UV-C light. One head was designated for printing polyurethane, a flexible and biocompatible polymer, to achieve biomimicry. The other head was loaded with a mixture of 250,000 cells per scaffold and GelMA/gelatin bioink containing the produced capsules for each sample (12 x 12 x 1 mm) (Figure 2.6). Scaffolds were divided into 2 groups for controlled comparison. In the control group, only standard expansion media was used, while in the experimental group, the produced capsules were added, and standard expansion media was used. The experiment lasted 14 days and the media was renewed every other day.

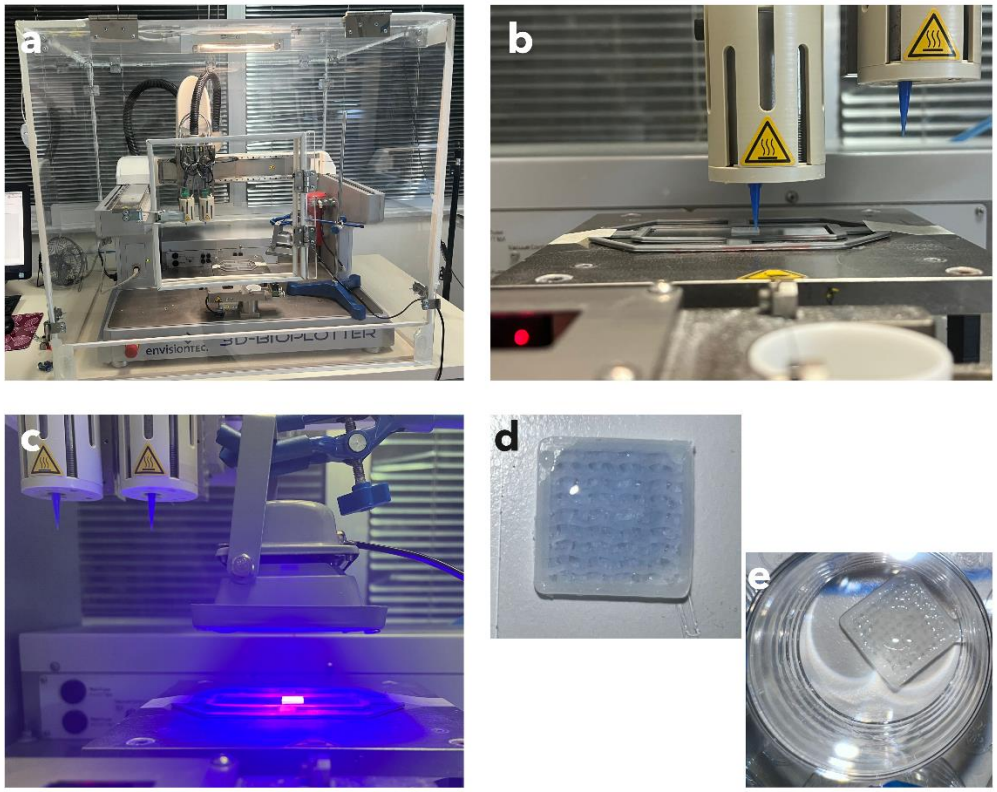

Figure 2.6 3D bioprinting process of the scaffolds (a) 3D bioprinting and cross-link setup, (b) printing process of scaffold, (c) cross-linking process of GelMA, (d) final scaffold (for visualization Trypan Blue is added to GelMA bioink.), (e) final scaffold with cells and capsules

2.2.8 Determination of cell numbers and morphology in scaffolds

The Alamar Blue test was employed to evaluate the viability of the cells in the scaffold during the cell culture period. The scaffolds were extracted from the medium and rinsed with PBS buffer in this experiment. The Alamar Blue solution was heated to 37ºC after being prepared as a 5% by volume solution in colorless low glucose DMEM 30 minutes prior. The heated solution was added to the wells of the cleansed samples in a volume of 2 ml. The samples were incubated in an incubator at 37ºC and 5% CO2 for 1 hour in the dark. At the conclusion of the period, 200 µl of the test sample was removed from each well and transferred to 96-well microplates. Each sample consisted of three biological and three technical replicates. The absorbance measurements were conducted at 570nm-595nm wavelengths after the 96-well microplate was inserted into the microplate reader. After the PBS wash of the samples, the Alamar Blue solution in the 12-well containers was removed. Subsequently, the wells were re-filled with new medium, and the culture

was maintained using the same samples. Alamar Blue tests could be conducted on the third, seventh, and fourteenth days using identical samples as a result of this Alamar Blue test feature. The calibration curve for ASC cells was employed to convert the values to obtain the cell numbers (Yilgor et al., 2009).

Samples were stained with Phalloidin/DAPI on days 3, 7, and 14 to assess cell morphology. Phalloidin was used to visualize actin filaments, while DAPI highlighted nuclei. The samples designated for staining were transferred to sterile wells, rinsed with PBS, and then fixed with a 3.7% (w/v) formaldehyde solution. After fixation with formaldehyde for 90 minutes under moderate shaking at room temperature, the samples were washed twice with PBS for 5 minutes each. Subsequently, the samples were treated with 0.1% (v/v) Triton X-100 at room temperature for 5 minutes to improve dye permeability. To prevent nonspecific binding, the samples were incubated with 1% BSA at 37°C for 2 hours. Following this, a phalloidin solution (1:1000 in 0.1% BSA) was added, and the samples were incubated at 37°C for 1 hour. The samples were then rinsed with PBS and treated with a DAPI solution (1:1000) at room temperature for 10 minutes. Finally, the samples were rinsed again with PBS, and cell morphology and proliferation were analyzed using an inverted fluorescence microscope (Zeiss Axio Observer Z1).

2.2.9 Immunofluorescent staining

On the third, seventh, and fourteenth days of the culture, the samples were fixed with 3.7% PFA for 90 minutes. Subsequently, they were rinsed with PBS for three 30-minute periods. CD31 (rabbit anti-CD31, Abcam) was employed as the primary antibody for immunofluorescence staining. In order to prevent non-specific adsorption to sections and permeabilize cell membranes, incubation was conducted for 2 hours at 4°C in PBS containing 0.1% Tween20 and 1% BSA. Samples were maintained at 4°C overnight following permeabilization and blocking, and primary antibody staining was performed. Secondary antibody staining is performed after 18 hours. Ultimately, the samples were treated with DAPI and kept at ambient temperature for 10 minutes. The samples were washed with PBS and viewed using an inverted fluorescence microscope.

2.2.10 Statistical analysis

The mean ± standard deviation (n=3) is the unit of measurement for all quantitative results. The data were analyzed using one-way or two-way ANOVA, with p-values less than 0.05 regarded as statistically significant. In instances where there were three or more groups, the Tukey test was implemented, while the t-test was employed in other instances to ascertain the significance of the distinction between various groups. The GraphPad Prism 10.0 software was employed to conduct the analyses.

3. RESULTS & DISCUSSION

3.1 Production of Capsules

The production of capsules was carried out with a concentration of 10% PCL (w/v) due to both the stability of the capsule dimensions and the success in release studies, the success of the determined values has been shown in previous studies (Goker et al., 2024). SEM visualizations of the produced capsules and scaffolds phases are shown in figure 3.1. Average capsule diameter is calculated with ImageJ software from the figure and found 1200 ± 100 nm.

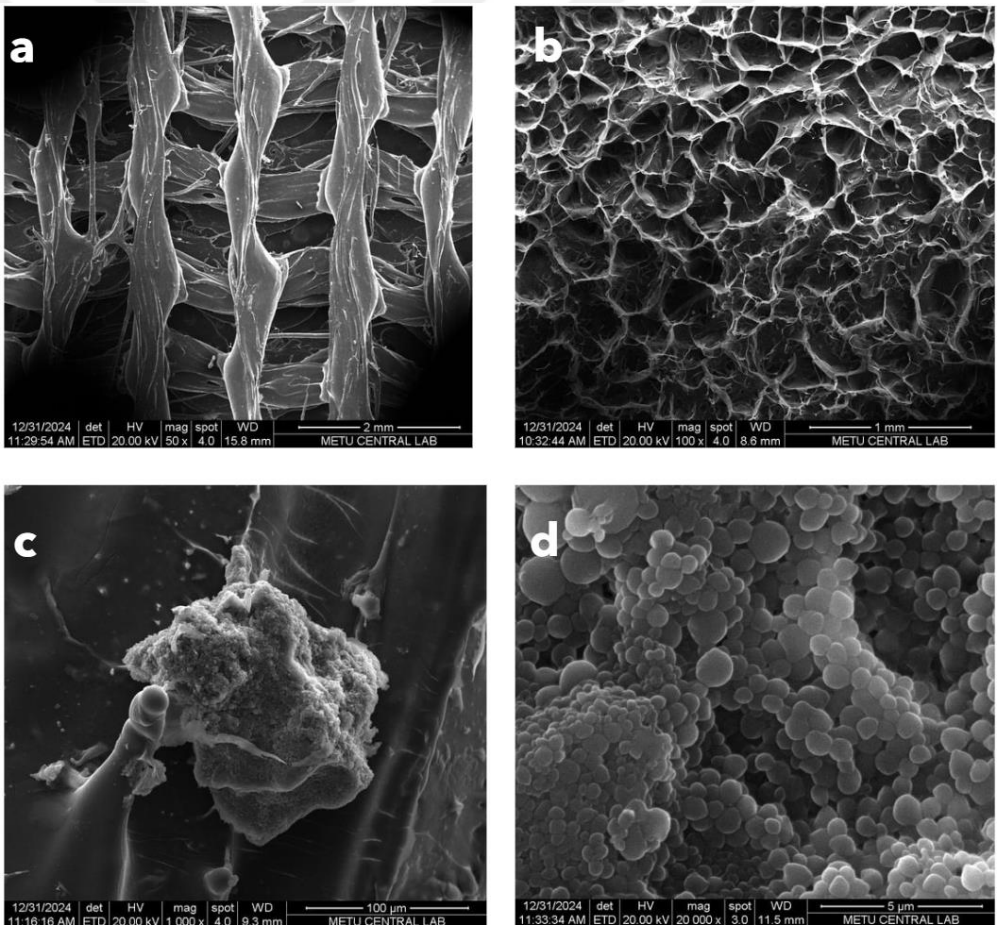

Figure 3.1 SEM images of capsule-embedded TPU/GelMA scaffolds (a) TPU only, 50x, (b) GelMA only, 100x, (c) capsules in scaffold, 1000x, (d) capsules only, 20000x

3.2 Release Profile of Capsules

The release profile of TGF-β1 and VEGF from growth factor-loaded capsules over 21 days from the scaffolds are determined by ELISA demonstrates a sustained delivery system that supports both proliferation and differentiation of ASCs into endothelial cells. TGF-β1 exhibited a rapid initial release during the first 7 days, reaching approximately 25%, followed by a gradual release, culminating in a cumulative release of about 40% by day 21 (Figure 3.2). Similarly, VEGF displayed an initial burst release of around 20% in the first week, with a steady release reaching nearly 30% by day 21 (Figure 3.3). The early burst release of VEGF likely enhances ASC proliferation through activation of VEGF receptor-mediated signaling, which is critical for angiogenesis and cellular expansion. Meanwhile, the sustained release of TGF-β1 over the 21-day period facilitates the differentiation of ASCs into endothelial cells by promoting vascular lineage commitment through SMAD-dependent pathways and regulation of endothelial-specific gene expression. VEGF also contributes to endothelial cell maturation and stabilization of nascent vascular structures.

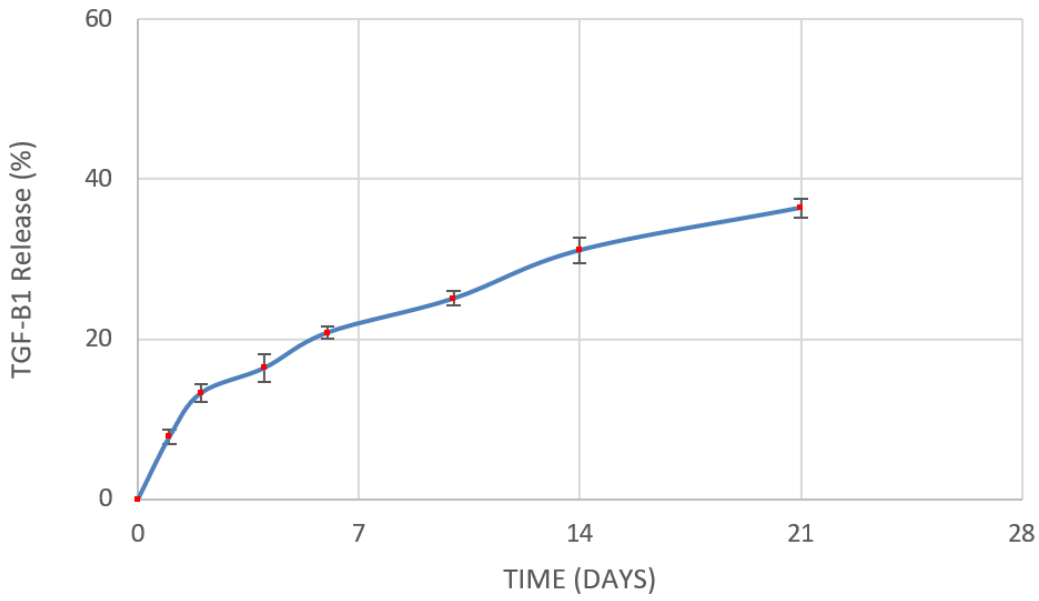

Figure 3.2 TGF-B1 release profile from scaffold in different time stamps

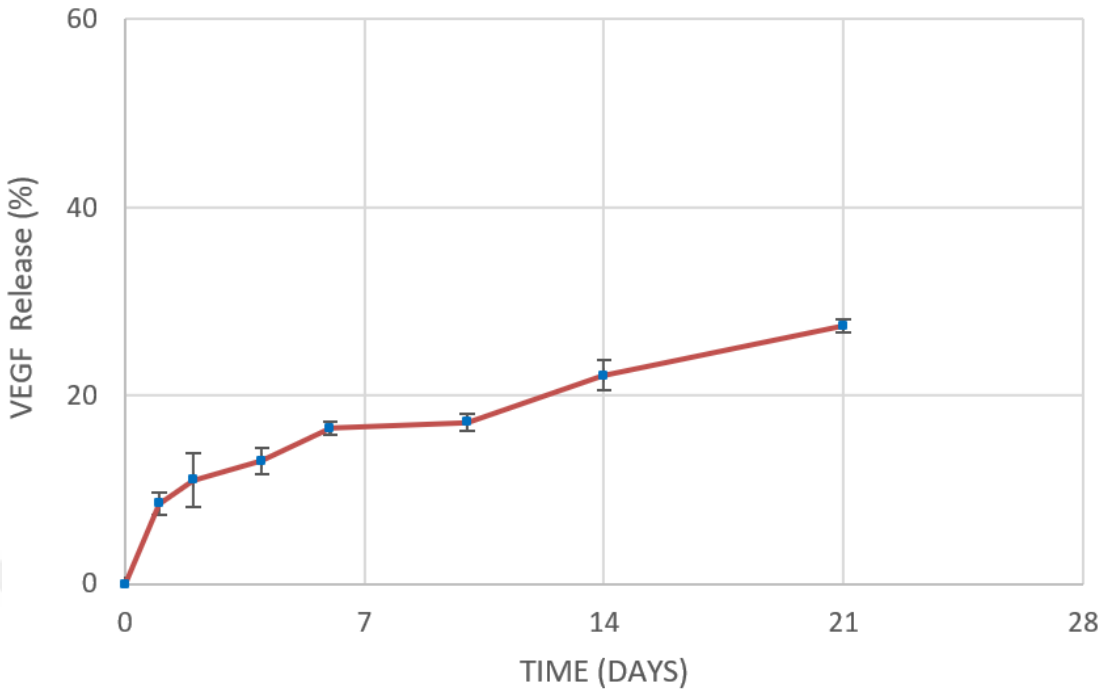

Figure 3.3 VEGF release profile from scaffold in different time stamps

3.3 Scaffold Optimizations

The concentration optimizations of GelMA/gelatin bioink and TPU ink to be used in the experiments and the internal structure and dimensions of the scaffold to be produced were decided by various trials.

3.3.1 GelMA/Gelatin bioink concentration optimizations

The degree of methacrylation (DM) of synthesized GelMA was determined by high-resolution proton nuclear magnetic resonance (1H-NMR) spectrometer (Bruker DPX 400) at the 1H resonance frequency of 400 MHz. The degree of methacrylation of GelMA was found to be 98.48% (Figure 3.4).

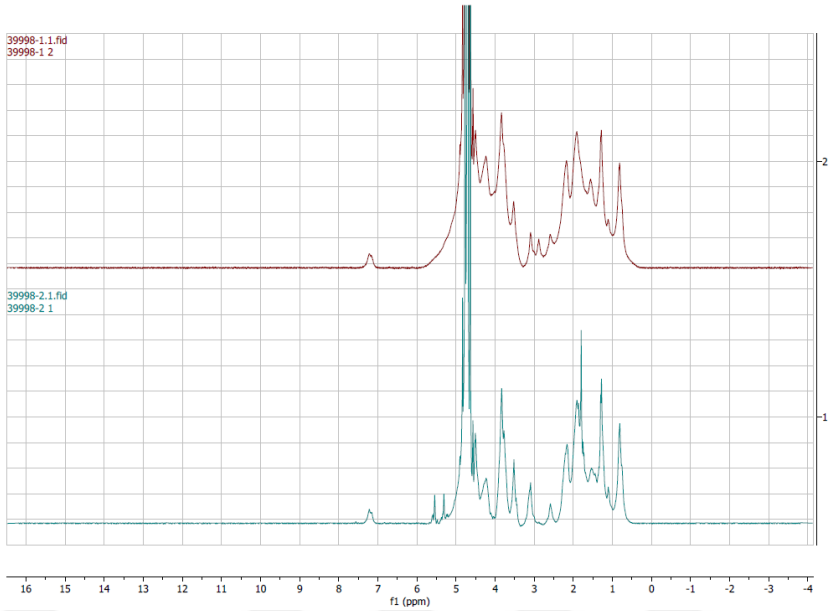

Figure 3.4 NMR result of GelMA

Printing experiments were performed using a 22 Gauge (0.413 mm) needle on the Envisiontech Bioplotter. Printing parameters obtained for various concentrations are shown in Table 3.1.

Table 3.1 GelMA/Gelatin printing parameters

Parameters	Value
GelMA concentration (w/v)	2-8
Gelatin concentration (w/v)	5-20
Pressure (Bar)	0.1-2
Bioink Temperature (°C)	20-25
Table Temperature (°C)	10-15
Print Speed (mm/sec)	2-8
UV application time (sec)	40 seconds

The scaffolds manufactured after the trials were evaluated and their printabilities were compared in Figure 3.5.

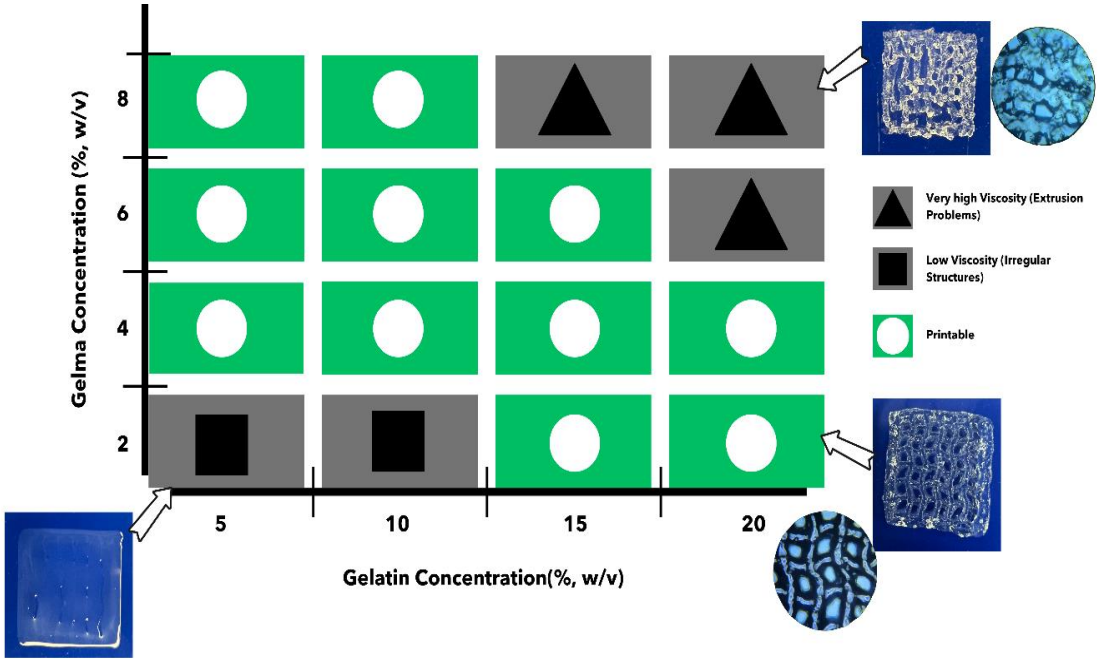

Figure 3.5 Print optimization of GelMA/Gelatin bioink

As a result of the data obtained, it was decided to use 5% (w/v) GelMA + 8% gelatin (w/v) + 0.5% (w/v) LAP concentration for the effect on cell proliferation and viability and printing stability to be used in the experiments.

3.3.2 Printing optimization of Polyurethane/Tetrahydrofuran ink

After the mixtures became homogeneous, they were loaded into the printer using a syringe and printing tests were performed. Printing tests for different concentrations are shown in Figure 3.6.

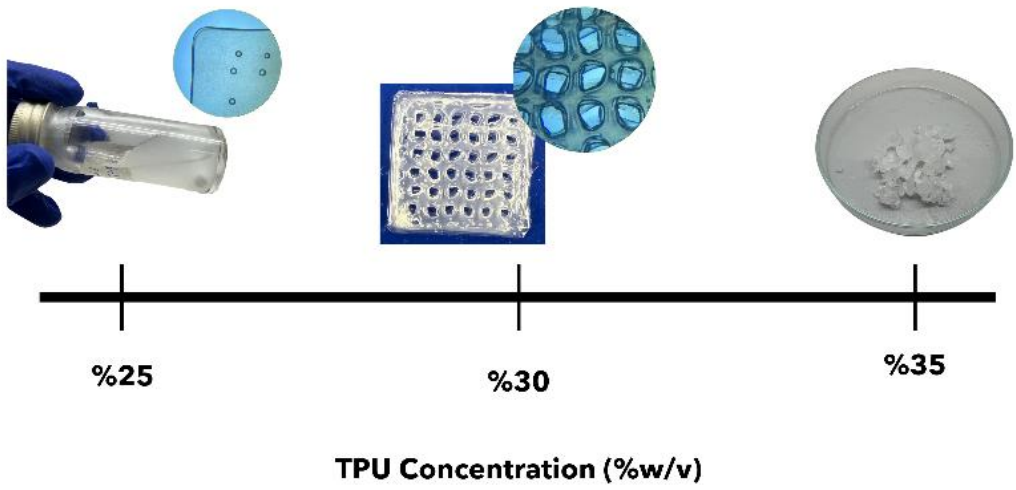

Figure 3.6 TPU concentration optimization

After the printing trials, it was observed that the mixture at concentrations of 25% w/v and below failed to protect the patterns created due to very low viscosity, while concentrations of 35% w/v and above experienced extrusion problems due to very high viscosity. For this reason, the optimal concentration for printing was selected as 30% w/v and the printing parameters are shared in Table 3.2.

Table 3.2 TPU ink printing parameters

Parameters	**Value**
TPU concentration (w/v)	30
Pressure (Bar)	1.5
Bioink Temperature (°C)	30
Table Temperature (°C)	20
Print Speed (mm/sec)	6.5

Due to THF's boiling point of 66°C and high volatility, it tends to move away quickly after printing, and it is planned that it will not cause any cytotoxic effects during removal since it is not in direct contact with the cell. To examine this hypothesis, mechanical testing and cytotoxicity testing were applied to the produced scaffolds.

3.4 Mechanical Test Results of Produced Scaffolds

To produce TPU ink part of the concentration optimized scaffolds, mechanical tensile tests were applied to raw TPU material, TPU/THF mixture in mold form and 3 different patterned scaffold architectures for internal pattern optimization. The hypotheses tested here are to see the change in mechanical properties of TPU/THF mixture after THF removal and also to compare the mechanical properties of the productions of this mixture in different architectures. When Table 3.3' is examined, a small decrease in mechanical properties of this mixture compared to raw TPU due to THF removal is observed, and the obtained values still meet the mechanical property range in the aim of the thesis. In Table 3.4, mechanical values of scaffolds produced in different architectures but with the same porosity are given. It was decided that all 3 designs met the desired properties mechanically, and the selected design was evaluated in terms of biomimicry. The wavy scaffolds irregular, organic architecture closely mimics the anisotropic and viscoelastic properties of aortic valves, promoting better integration with native tissue. The interconnected, multi-directional pores facilitate enhanced cellular adhesion, proliferation, and migration, creating an environment conducive to tissue regeneration. Additionally, the wavy structure optimizes nutrient and oxygen diffusion while efficiently removing metabolic waste, ensuring cell viability. Unlike line or triangular patterns, the wavy design balances structural integrity with the biological demands of tissue growth and remodeling, making it ideal for applications requiring functional and anatomical biomimicry, such as aortic valve scaffolds. Therefore, it was decided to move on to cell culture experiments with a wavy design scaffold.

Table 3.3 Mechanical test results

	TPU	**TPU Ink**
Maximum Tensile Strength (MPa)	34.325 ±5.386	28.558 ±3.778
Percentage Elongation (%)	598.865 ±10.235	501.233 ±12.321
Young Modulus (MPa)	20.113±1.389	17 .897±2.901

Table 3.4 Different designs of scaffolds and their mechanical properties

Sample Image	Scaffold Architecture	Mechanical Test Results
	Design: Wave Porosity: %60	**Maximum Tensile Strength (MPa):** 28.986±4.112 **Percentage Elongation (%):** 500.998 ±14.667 **Young Modulus (MPa):** 18.571±3.109
	Design: Lines Porosity: %60	**Maximum Tensile Strength (MPa):** 25.322± 3.753 **Percentage Elongation (%):** 501.576±10.856 **Young Modulus (MPa):** 19.567±4.028
	Design: Triangles Porosity: %60	**Maximum Tensile Strength (MPa):** 26.608±5.976 **Percentage Elongation (%):** 502.085±15.533 **Young Modulus (MPa):** 18.989±3.850

3.5 Scaffold Inner Pattern and Dimensions

Aortic valve tissue scaffolds need to have wavy inner patterns to resemble the natural structure and biomechanics of the native valve leaflets. The crimped or undulated collagen fibrils help the valve handle the repeated stress it faces during the heart's pumping action. The wavy design of the architecture allows the scaffold to stretch and rebound effectively, spreading out mechanical stress evenly across the leaflet. Also, the wavy design helps cells adhere and line up correctly, which supports the remodeling of the extracellular matrix and promotes the development of a functional, living valve tissue as time goes on. Creating these detailed patterns is crucial for developing bioengineered valves that fit smoothly into the ever-changing environment of the heart. Because of that reason the selected pattern dimensions and orientation is given below in Figure 3.7.

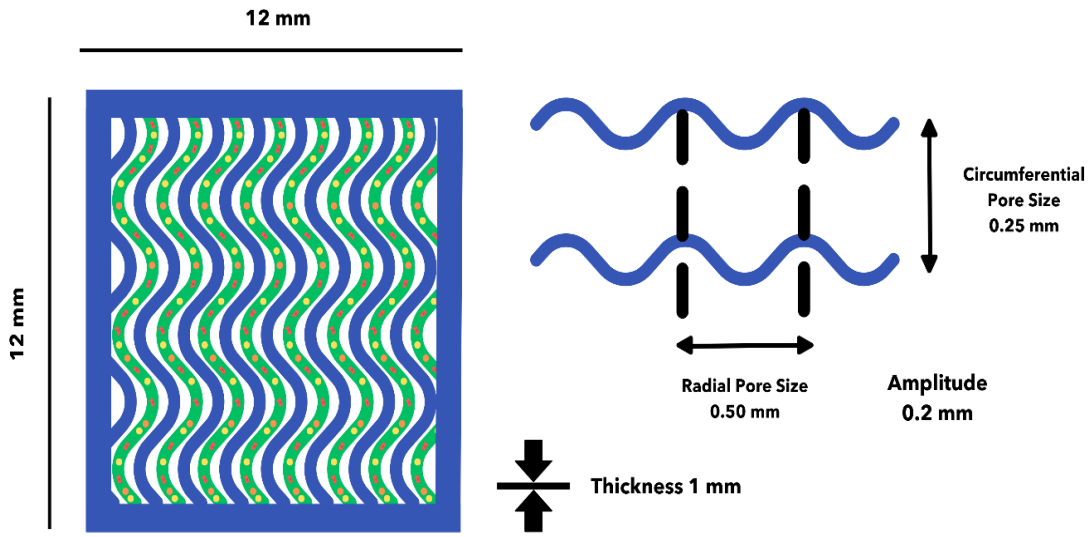

Figure 3.7 Inner pattern and dimensions of manufactured scaffold

3.6 Cytotoxicity Test Results

The cytotoxicity properties of the synthesized TPU1 and TPU60 samples were investigated by indirect toxicity test. After 24, 48 and 72 hours of addition of extraction fluid, the cell layer spread and the number of dead cells according to the experimental groups were examined with a light microscope at 10x magnification. The cell layer spread observed at 24, 48 and 72 hours is given in Figure 3.8. The changes observed in cell morphology throughout the culture were examined at 40x magnification and the results are presented in Figure 3.9. Figure 3.10. shows the cell number and inhibition according to Alamar Blue test results.

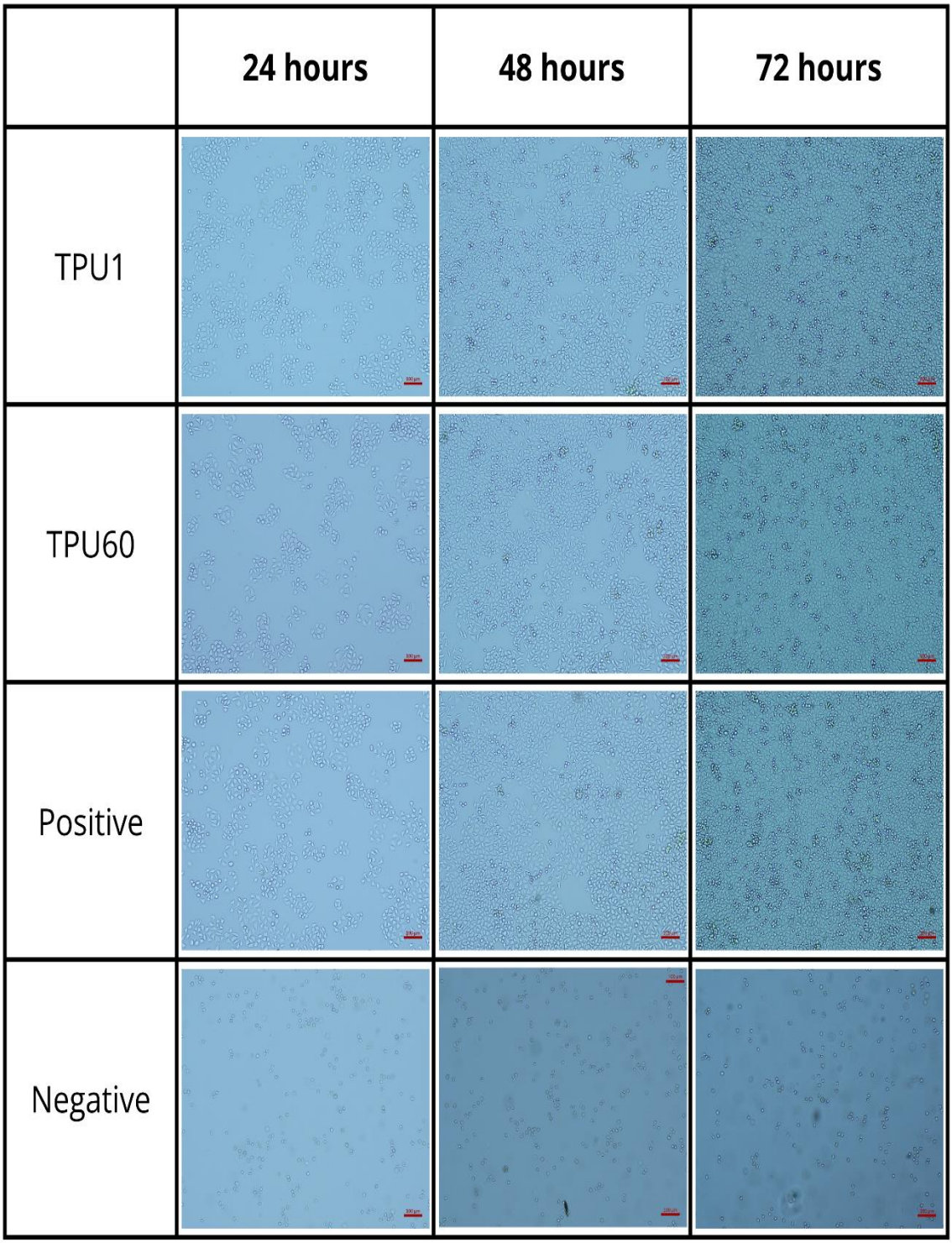

Figure 3.8 The change in cell layer spread according to experimental groups at 24, 48 and 72 hours after addition of extraction fluid (10x)

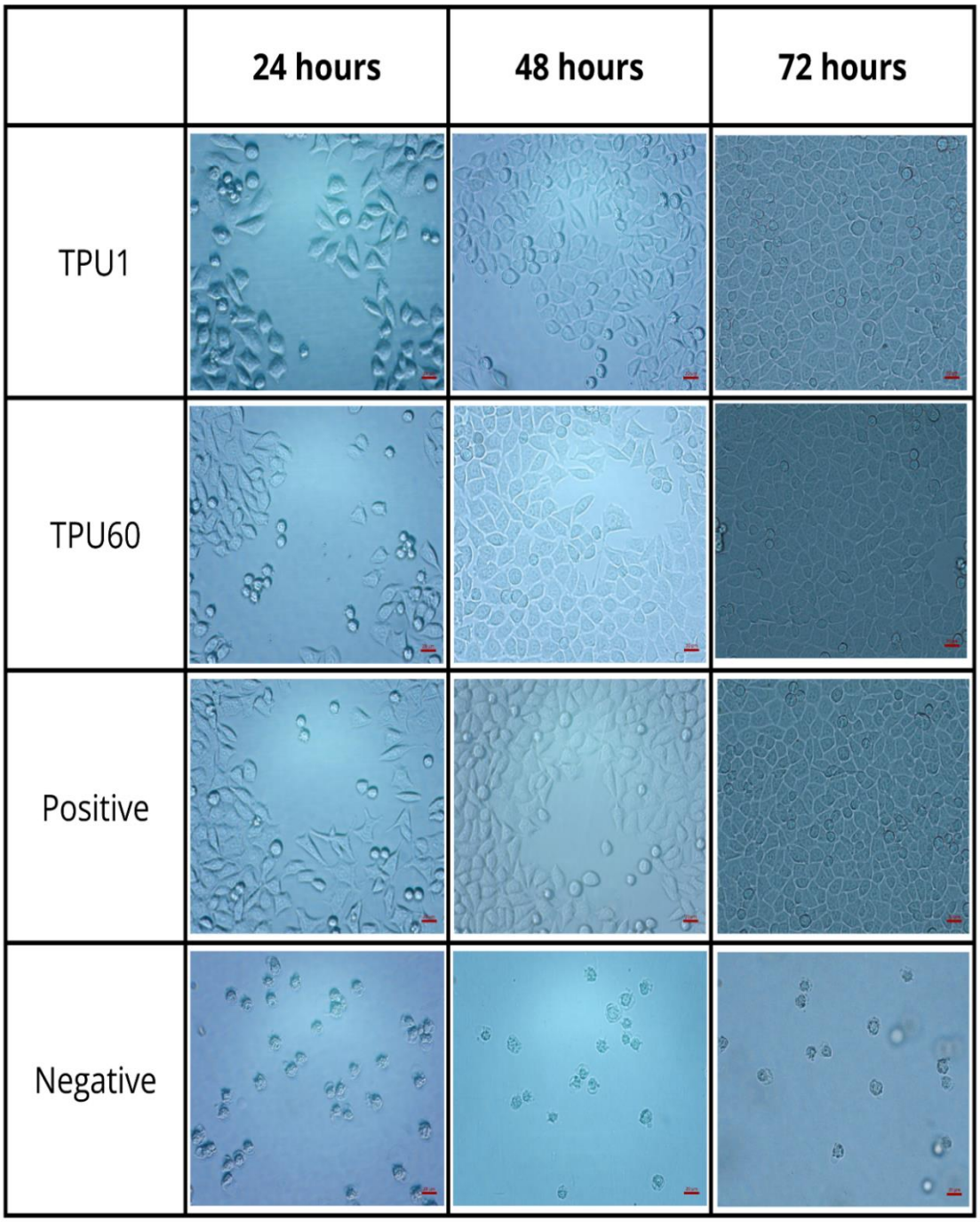

Figure 3.9 Change in cell morphology according to experimental groups at 24, 48 and 72 hours after addition of extraction fluid (40x)

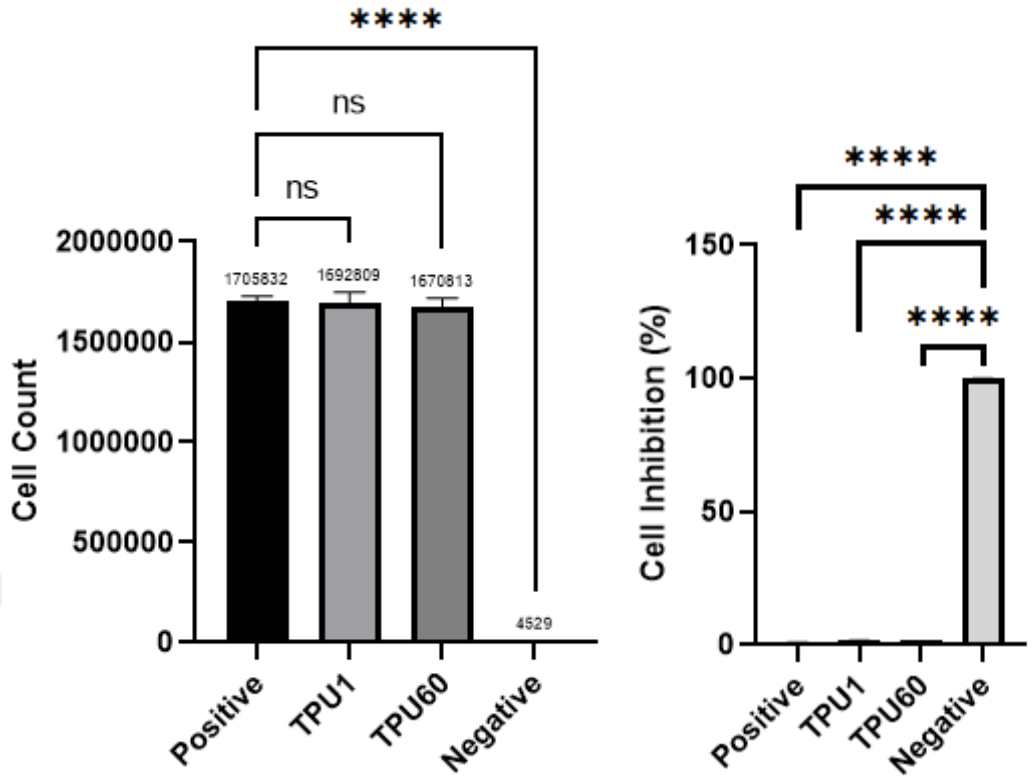

Figure 3.10 The change in the number of viable cells and the degree of inhibition across experimental groups was assessed 72 hours after the addition of the extraction fluid, with results normalized to the negative control (**** P < 0.0001)

According to the results of microscopic examination and cell counting, the results of the experimental groups according to the "cytotoxicity test evaluation criteria" scoring table are presented in Table 3.5.

Table 3.5 Cytotoxicity test evaluation criteria

	Group	Score		Group	Score
Confluency	TPU1	1	**Change in cell morphology**	TPU1	1
	TPU60	1		TPU60	1
Number of dead cells (Floating cells)	TPU1	1	**Cell growth inhibition**	TPU1	0
	TPU60	1		TPU60	0

According to these results, the cytotoxic response index and cytotoxicity evaluation results for the produced materials are presented in Table 3.6. Accordingly, TPU1 and TPU60 are biocompatible.

Table 3.6 Cytotoxicity assessment results for TPU1 and TPU60

Group	Cytotoxic response index	"Material is Cytotoxic"
TPU1	1	NO
TPU60	1	NO

3.7 Cell Viability Results

Figure 3.11 shows the results of cell viability for ASCs that were placed on hybrid scaffolds, highlighting the differences between groups that had growth factor-loaded capsules and those that did not. Evaluation was done for ASCs viability by using the Alamar Blue Assay over a 14-day culture period. The assay results show that both groups successfully adhered to the scaffold surface and consistently grew over the course of the experiment. These growth factors play important roles in managing how cells behave, which is crucial for tissue engineering tasks. VEGF plays a crucial role in stimulating the formation of new blood vessels, ensuring that developing tissues receive adequate nutrients and oxygen. On the other hand, TGF-β1 helps with cell growth, differentiation, and the creation of the matrix, which supports the integration of scaffolds and helps regenerate functional tissue. The growth factors in the capsules were shown to create a supportive environment that helped the ASCs survive and grow.

When the cell counts on the 14th day were examined, it was observed that the control group and the capsule group were equal compared to the 3rd and 7th days. The reason for this is hypothesized to be based on the morphologies observed in both SEM images, DAPI-Phalloidin images and CD-31 results, where the adipose-derived stem cells in the

capsule groups are thought to enter the endothelial cell differentiation pathway due to TGF-β1 and VEGF growth factors, leading to a decrease in their proliferation.

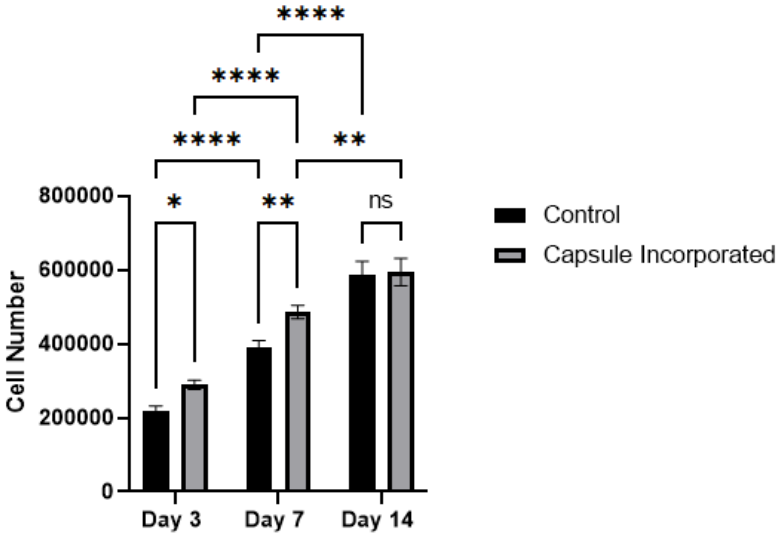

Figure 3.11 Cell viability results of ASCs seeded on scaffolds were determined using the Alamar Blue assay. The data, presented as the number of viable cells, are expressed as the mean ± standard deviation from three independent experiments (* $P < 0.05$, ** $P < 0.01$, *** $P < 0.001$, **** $P < 0.0001$)

3.8 Cell Morphology Results

To examine the morphology of the cells on the scaffold, samples from both groups on days 3, 7 and 14 were examined by SEM imaging (Figure 3.12). Cell orientation and cell morphology of the encapsulated group compared to the control group indicate that ASCs are at the beginning stage of endothelial cell differentiation in the 14th day samples (Figure 3.13).

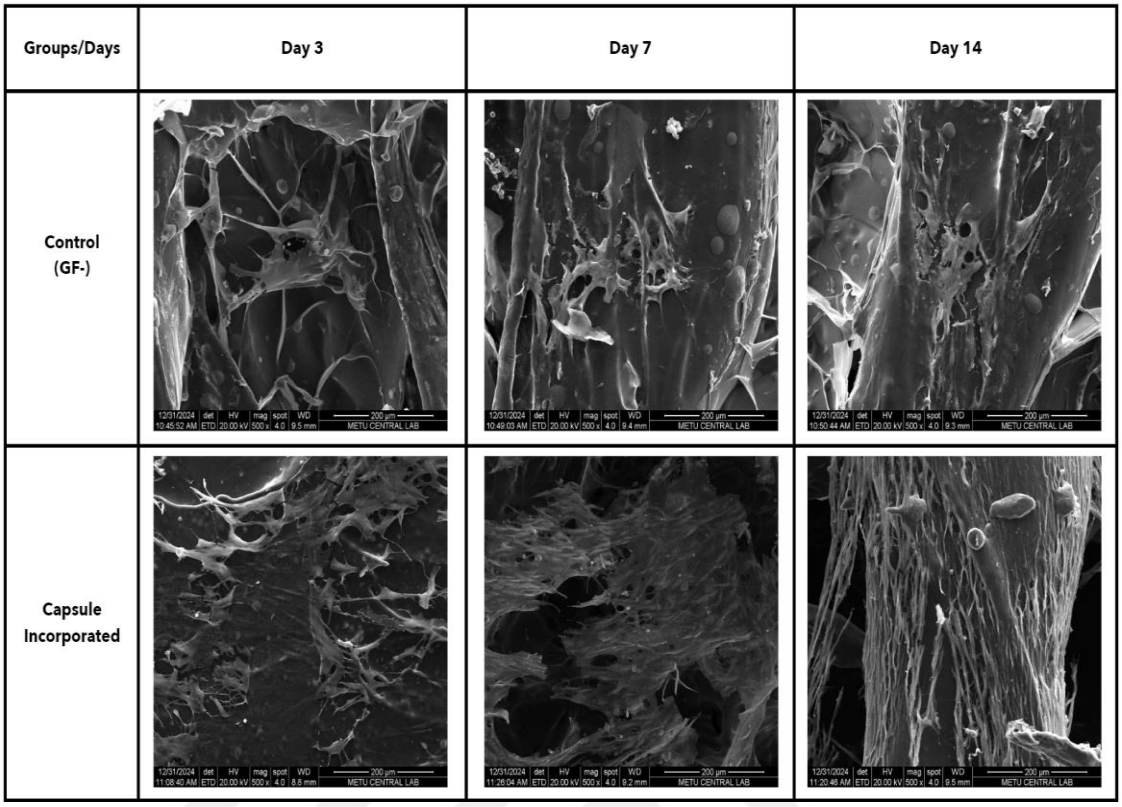

Figure 3.12 SEM images of groups on different days. Images were taken under 500x magnification scale bar = 200 μm

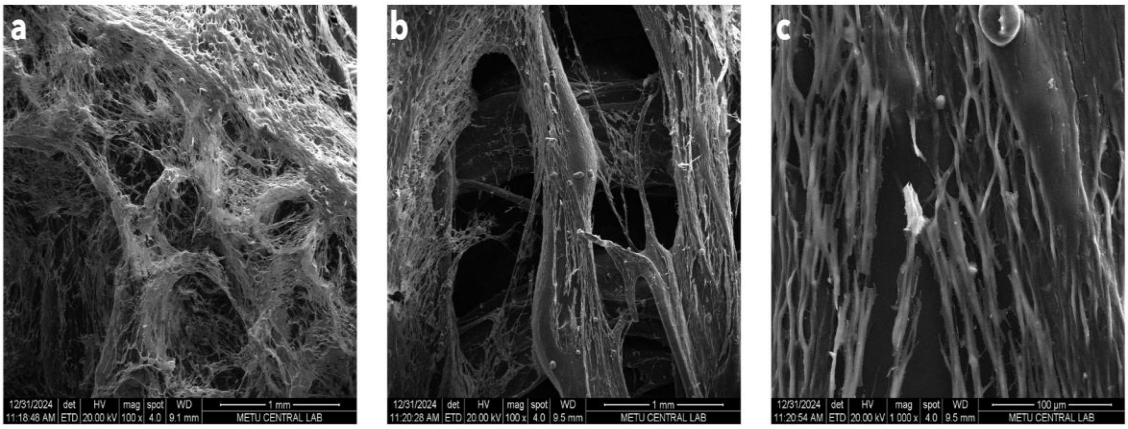

Figure 3.13 SEM images of samples from the capsule-incorporated group on day 14 were captured at (a) and (b) 100x magnification, and (c) 1000x magnification to examine cell attachment and morphology within the fibers of TPU and GelMA

Phalloidin-DAPI staining was applied to examine the morphological distribution of the cells, and 5X (Figure 3.14) and 10X (Figure 3.16) images and staining intensity graphs

(Figure 3.15 and 3.17,) of both groups under the fluorescent microscope were given. It was observed that the increase in cell count in the encapsulated group was higher compared to the control group until the 14th day, and since the cells in the 14th day groups started to differentiate into the endothelial cell structure found in the aortic valve structure, they were equal to the control group samples in cell proliferation. This situation was also observed in the Alamar Blue test results.

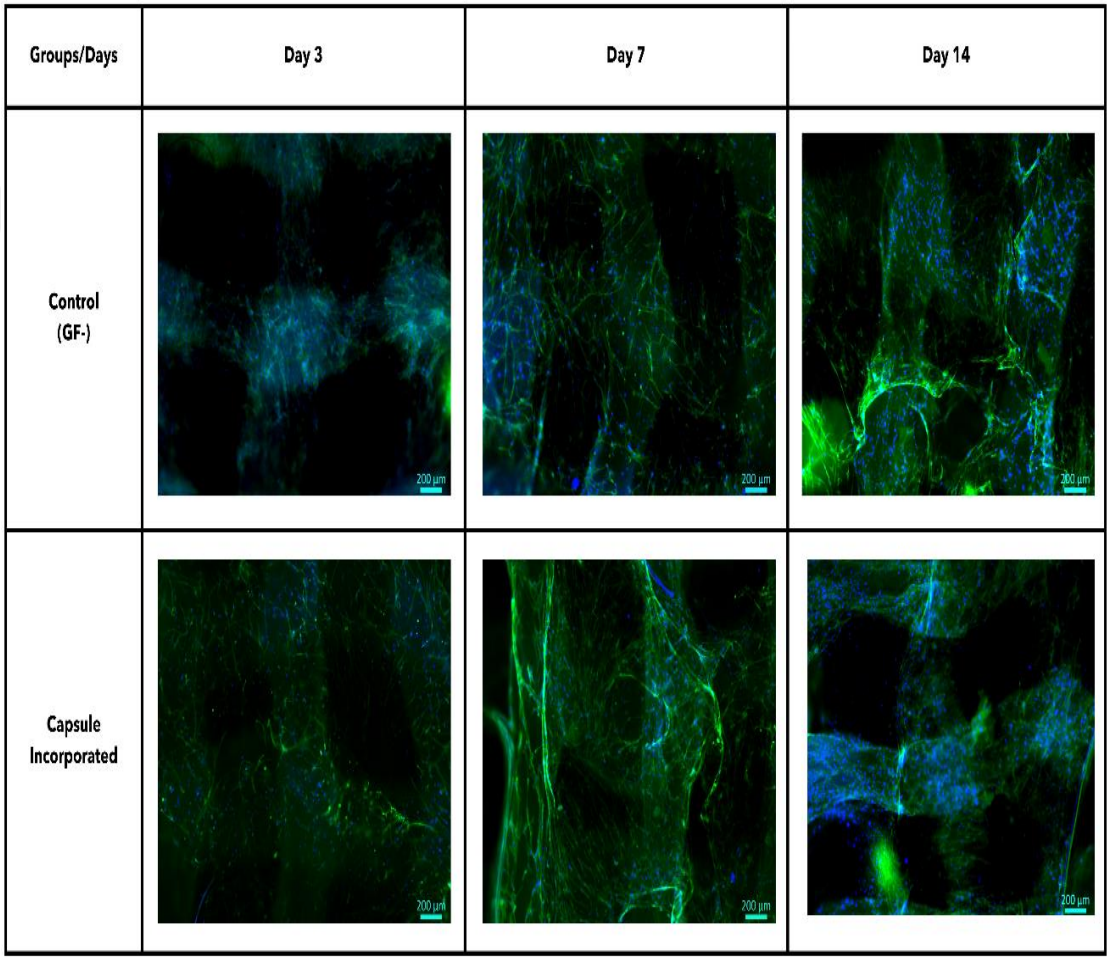

Figure 3.14 DAPI-Phalloidin staining of both groups under 5X magnification (Scale bar = 200 µm). Channels; blue: DAPI, green: Phalloidin

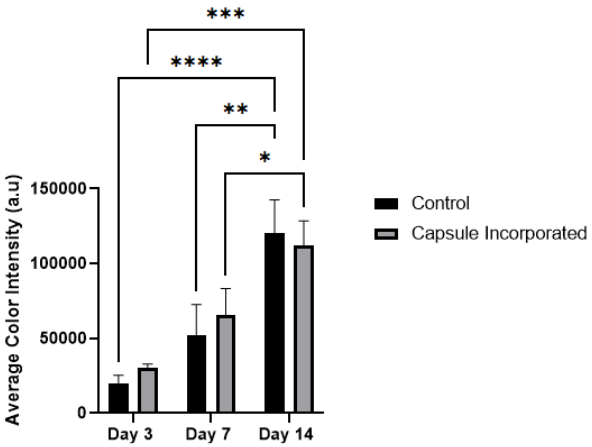

Figure 3.15 The graph of average color intensity comparison between the control group and the capsule-incorporated scaffolds, shown in figure 3.14 (* $P < 0.05$, ** $P < 0.01$, *** $P < 0.001$, **** $P < 0.0001$)

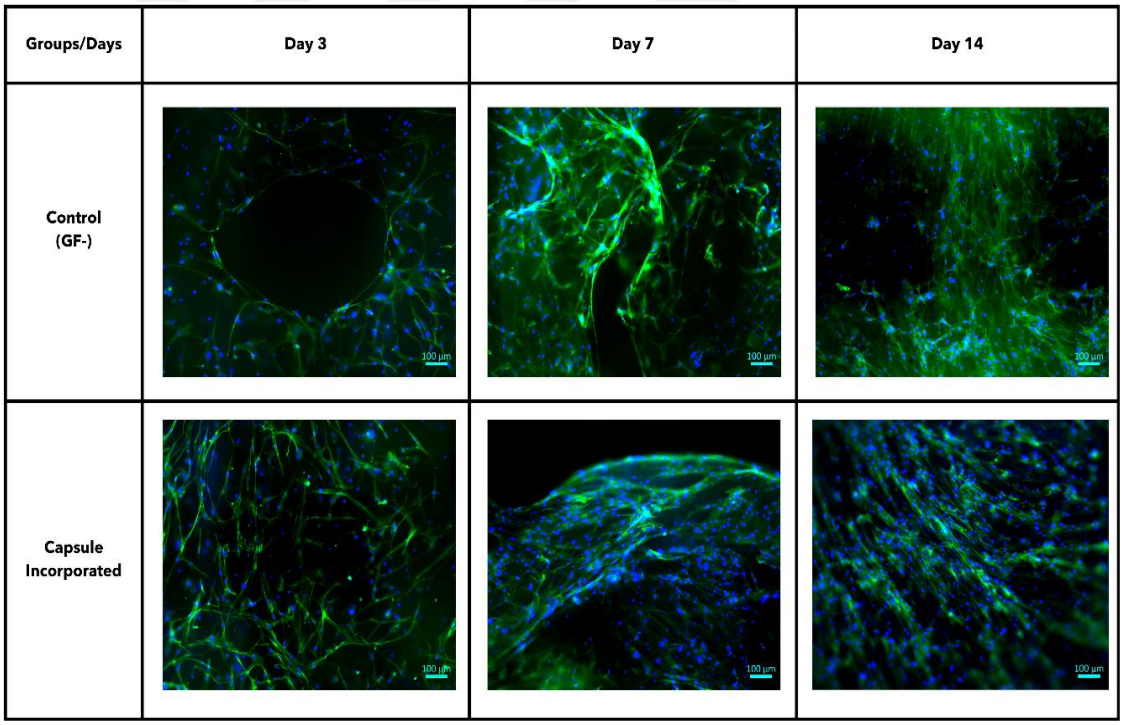

Figure 3.16 DAPI-Phalloidin staining of both groups under 10X magnification (Scale bar = 100 μm). Channels; blue: DAPI, green: Phalloidin

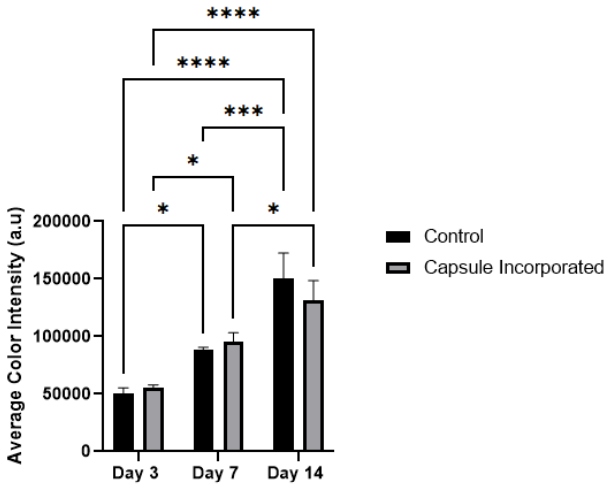

Figure 3.17 The graph of average color intensity comparison between the control group and the capsule-incorporated scaffolds, shown in figure 3.16 ($P < 0.05$, ** $P < 0.01$, *** $P < 0.001$, **** $P < 0.0001$)

3.9 Immunofluorescent Staining Results

CD31, also known as PECAM-1, is a glycoprotein expressed on endothelial cells and serves as a marker for endothelial differentiation. In the context of ASCs undergoing endothelial differentiation, CD31 staining is used to confirm the acquisition of an endothelial phenotype. Positive CD31 expression indicates that the MSCs are successfully differentiating into endothelial-like cells (Murphy Wang H. T. Nguyen T., 2020). When the experimental results were analyzed, fluorescence was observed in the CD-31 staining of the 14th-day samples in the capsule-incorporated group compared to 14. Day control group (Figure 3.18). This finding suggests that the shear stress provided by dynamic culture in future studies may increase cellular stress and promote greater cell differentiation. The limitations of static culture in mimicking the natural structure and the inadequacy of the culture duration for full differentiation have likely contributed to the observed staining findings not reaching definitive levels. In future studies, it will be possible to obtain clearer results by evaluating the outcomes of cultures performed in a pulsative bioreactor system and incorporating quantitative analyses.

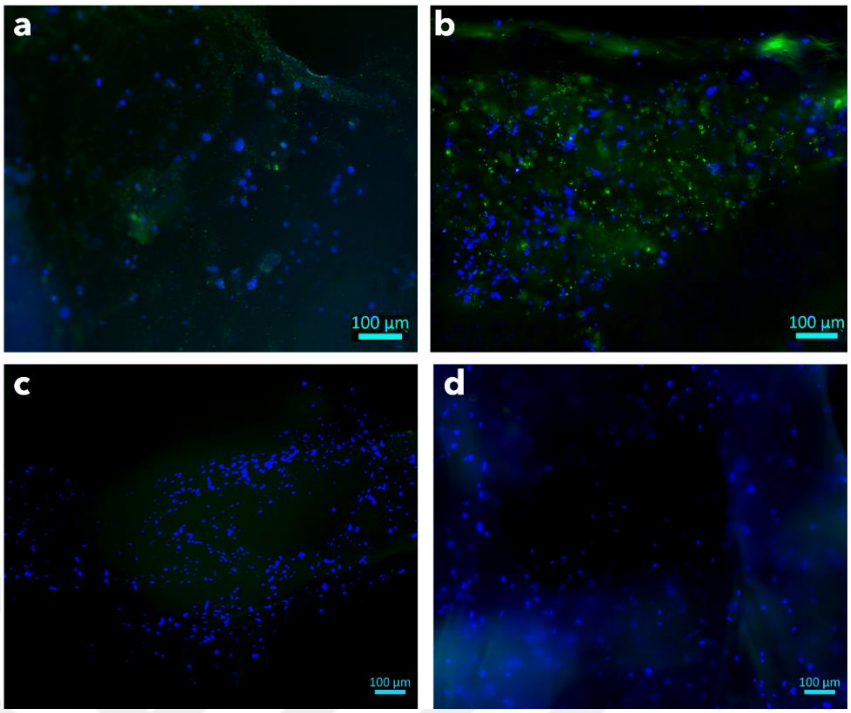

Figure 3.18 Fluorescence microscope images (10X) (a-b) capsule incorporated group, (c-d) control group. Channels; green: CD-31, blue: DAPI (Scale bar = 100 µm)

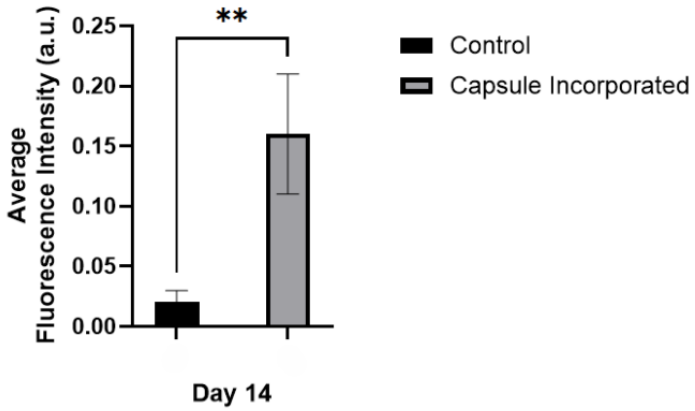

Figure 3.19 Graph showing the mean CD-31 signal intensity for the control group and the capsule-incorporated group on day 14 (** $P < 0.01$)

4. CONCLUSION

This thesis explores the creation of biomimetic aortic valve equivalents using cutting-edge 3D bioprinting techniques and new material formulations. By combining TPU with GelMA and gelatin-based hydrogels, scaffolds have customized mechanical properties, are biocompatible, and maintain structural integrity. By using controlled-release growth factors like VEGF and TGF-β1, the engineered scaffolds created a supportive environment for the adhesion, growth, and development of adipose-derived stem cells. This research highlights the possibilities of using stem cell-based tissue engineering to create living, functional heart valves that are created for individual patients. The tests on the scaffolds showed that they can handle physiological pressures and mimic the unique mechanical properties of natural aortic valves. Material concentrations and printing parameters to produce the two-phase scaffold were optimized by taking help from both the various experimental results and the literature. Additionally, the cytotoxicity tests showed that the materials are biocompatible, indicating that the scaffolds didn't cause any negative reactions in cells, which supports their use in biomedical applications. This research really stands out because of the unique dual-phase structure of the scaffold. It combines the strong mechanical properties of TPU with the biological benefits of GelMA and gelatin hydrogels. This method not only copies the extracellular matrix but also promotes better cell interaction and helps with tissue regeneration. Adding VEGF and TGF-β1 really boosted the scaffolds' ability to regenerate by encouraging cells to grow and differentiate, which is essential for creating functional tissue. The 14-day lab study showed that the scaffolds could effectively support cell survival and growth. The group that included growth factors had notably better results for early signs of differentiation of endothelial cells which is crucial cell line while creating biomimic aortic valve substitutes. This thesis highlights important gaps in current heart valve replacement therapies from a clinical standpoint. The engineered heart valve scaffolds in this study present a hopeful alternative compared to traditional mechanical or bioprosthetic valves, which can't grow, adapt, or escape long-term issues like thrombosis or structural breakdown. This method uses a patient’s own stem cells along with customizable 3D printing, opening possibilities for specialized solutions that might lower the chances of immune rejection and improve long-term performance.

This study marks a crucial advancement in regenerative cardiovascular medicine. This sets strong groundwork for upcoming preclinical studies, like those involving animal models, to take a closer look at how these tissue-engineered heart valves perform and their safety over the long haul. Additionally, new developments in how scaffolds are made, like 4D bioprinting and computational modeling, are likely to improve the design and performance of future implants. To conclude, this research highlights how 3D bioprinting and tissue engineering could really change the game when it comes to tackling important issues in heart valve replacement. Ongoing collaboration between material science, bioengineering, and clinical research will play a key role in turning these discoveries into practical treatments, which could create a new approach to heart diseases related to valves.

Ongoing and Future Work: The study conducted in this thesis is a preliminary study of a personalized aortic valve approach that will be created with a 3D modeling and mathematical model planned to be cultured in a pulsating reactor system with dynamic culture method in future studies. The material characterized in this thesis was produced as a pilot in the complex aortic valve geometry and in future studies, it will be provided to differentiate into valve endothelial cell and valve interstitial cell structure found in the aortic valve by using only one type of stem cell with coaptation ability in 21 days of dynamic culture (Figure 4.1). The aim of the studies conducted in the thesis is to show that the characterized material and the growth factor encapsulation method used work effectively and to observe cell behavior, proliferation and initial differentiation findings.

Figure 4.1 Prototype aortic valve scaffold produced with 3D printing

REFERENCES

Ahmed et al., A. (2020). 4D bioprinting of adaptive tissue-engineered heart valves. *Nature Materials*. https://doi.org/10.1038/s41563-020-0708-8

Ahmed et al., A. (2024). Temporal trends and procedural safety of mitral valve transcatheter edge-to-edge repair in patients with previous CABG. Future Cardiology. https://doi.org/10.2217/fca-2023-0045

Alaribe, F. N., Manoto, S. L., & Motaung, S. C. K. M. (2016). Scaffolds from biomaterials: Advantages and limitations in bone and tissue engineering. Biologia, 71(4), 353–366. https://doi.org/10.1515/biolog-2016-0056

Al-Atassi, T., Toeg, H. D., Jafar, R., Sohmer, B., Labrosse, M., & Boodhwani, M. (2015). Impact of aortic annular geometry on aortic valve insufficiency: Insights from a preclinical, ex vivo, porcine model. The Journal of Thoracic and Cardiovascular Surgery, 150(3), 656-664.e1. https://doi.org/10.1016/j.jtcvs.2015.06.060

Augustine, R., Gezek, M., Nikolopoulos, V. K., Buck, P. L., Bostanci, N. S., & Camci-Unal, G. (2024). Stem Cells in Bone Tissue Engineering: Progress, Promises and Challenges. Stem Cell Reviews and Reports, 20(7), 1692–1731. https://doi.org/10.1007/s12015-024-10738-y

Badylak Taylor D. Uygun K., S. F. (2009). Whole-organ tissue engineering: Decellularization and recellularization of three-dimensional matrix scaffolds. Annual Review of Biomedical Engineering, 13, 27–53. https://doi.org/10.1146/annurev-bioeng-071910-124743

Bajaj, P., Schweller, R. M., Khademhosseini, A., West, J. L., & Bashir, R. (2014). 3D Biofabrication Strategies for Tissue Engineering and Regenerative Medicine. Annual Review of Biomedical Engineering, 16(1), 247–276. https://doi.org/10.1146/annurev-bioeng-071813-105155

Bhattarai, N., Edmondson, D., Veiseh, O., Matsen, F. A., & Zhang, M. (2005). Electrospun chitosan-based nanofibers and their cellular compatibility. Biomaterials, 26(31), 6176–6184. https://doi.org/10.1016/j.biomaterials .2005.03.027

Blanpain Fuchs E., C. (2009). Epidermal stem cells of the skin. Annual Review of Cell and Developmental Biology, 25, 515–539. https://doi.org/10.1146/annurev .cellbio.042308.113234

Chen Liu X., F. M. (2017). Advancing biomaterials of human origin for tissue engineering. Progress in Polymer Science, 53, 86–168. https://doi.org/10.1016/j.progpolymsci.2015.04.003

Dasi Ge L. Sotiropoulos F. Yoganathan A. P., L. P. (2009). Vorticity dynamics of aortic valve leaflet motion: An in vitro analysis of the biological and mechanical implications. Journal of Biomechanics, 42(1), 32–39. https://doi.org/10.1016/j.jbiomech.2008.10.024

Ehrlich, H. (2019). Biomaterials and biological materials for tissue engineering. In Springer. https://doi.org/10.1007/978-3-319-92483-0_1

Engelhardt, S., Sauerzapf, S., Preim, B., Karck, M., Wolf, I., & De Simone, R. (2019). Flexible and comprehensive patient-specific mitral valve silicone models with chordae tendineae made from 3D-printable molds. International Journal of Computer Assisted Radiology and Surgery, 14(7), 1177–1186. https://doi.org/10.1007/s11548-019-01971-9

Engin and Güvenç O., M. (2024). Transcatheter aortic valve implantation in young patients: Why, for what? Polish Heart Journal. https://doi.org/10.5603/PHJ.a2024.001

Engler, D. A. (1996). Use of Vascular Endothelial Growth Factor for Therapeutic Angiogenesis. Circulation, 94(7), 1496–1498. https://doi.org/10.1161/01.CIR.94.7.1496

Ergene, E., Yagci, B. S., Gokyer, S., Eyidogan, A., Aksoy, E. A., & Yilgor Huri, P. (2019). A novel polyurethane-based biodegradable elastomer as a promising material for skeletal muscle tissue engineering. Biomedical Materials, 14(2), 025014. https://doi.org/10.1088/1748-605X/ab007a

Ferrara, N., Gerber, H.-P., & LeCouter, J. (2003). The biology of VEGF and its receptors. Nature Medicine, 9(6), 669–676. https://doi.org/10.1038/nm0603-669

Fidalgo, C., Iop, L., Sciro, M., Harder, M., Mavrilas, D., Korossis, S., Bagno, A., Palù, G., Aguiari, P., & Gerosa, G. (2018). A sterilization method for decellularized xenogeneic cardiovascular scaffolds. Acta Biomaterialia, 67, 282–294. https://doi.org/10.1016/J.ACTBIO.2017.11.035

Figliozzi et al., S. (2024). Cardiovascular magnetic resonance in patients with mitral valve prolapse. Journal of Cardiovascular Magnetic Resonance. https://doi.org/10.1186/s12968-024-00915-y

Fisher et al., J. (2024). Enhancing a journal's identity in tissue engineering. Political Studies Review. https://doi.org/10.1177/14789299241292570

Fraser Wulur I. Alfonso Z. Hedrick M. H., J. K. (2006). Fat tissue: An underappreciated source of stem cells for biotechnology. Trends in Biotechnology, 24(4), 150–154. https://doi.org/10.1016/j.tibtech.2006.01.010

Gao et al., X. (2024). Artificial heart valve scaffold based on electrospun PCL/PU three-layer composite fibers. Applied Sciences. https://doi.org/10.3390/app14020601

Ghosh, R. N., Thomas, J., B. R., V., N. G., D., Janardanan, A., Namboothiri, P. K., & Peter, M. (2023). An insight into synthesis, properties and applications of gelatin methacryloyl hydrogel for 3D bioprinting. Materials Advances, 4(22), 5496–5529. https://doi.org/10.1039/D3MA00715D

Gimble Katz A. J. Bunnell B. A., J. M. (2007). Adipose-derived stem cells for regenerative medicine. Circulation Research, 100(9), 1249–1260. https://doi.org/10.1161/01.RES.0000265074.83288.09

Goker, M., Derici, U. S., Gokyer, S., Parmaksiz, M. G., Kaya, B., Can, A., & Yilgor, P. (2024). Spatial Growth Factor Delivery for 3D Bioprinting of Vascularized Bone with Adipose-Derived Stem/Stromal Cells as a Single Cell Source. ACS Biomaterials Science & Engineering, 10(3), 1607–1619. https://doi.org/10.1021/acsbiomaterials.3c01222

Greiner, A., & Wendorff, J. H. (2007). Electrospinning: A Fascinating Method for the Preparation of Ultrathin Fibers. Angewandte Chemie International Edition, 46(30), 5670–5703. https://doi.org/10.1002/anie.200604646

Gu, Q., Tomaskovic-Crook, E., Lozano, R., Chen, Y., Kapsa, R. M., Zhou, Q., Wallace, G. G., & Crook, J. M. (2016). Functional 3D Neural Mini-Tissues from Printed Gel-Based Bioink and Human Neural Stem Cells. Advanced Healthcare Materials, 5(12), 1429–1438. https://doi.org/10.1002/adhm.201600095

Gudapati, H., Dey, M., & Ozbolat, I. (2016). A comprehensive review on droplet-based bioprinting: Past, present and future. Biomaterials, 102, 20–42. https://doi.org/10.1016/j.biomaterials.2016.06.012

Hanna et al., J. (2010). Direct reprogramming of terminally differentiated mature B lymphocytes to pluripotency. Cell, 133(2), 250–264. https://doi.org/10.1016/j.cell.2008.03.020

Hasan, A., Ragaert, K., Swieszkowski, W., Selimović, Š., Paul, A., Camci-Unal, G., Mofrad, M. R. K., & Khademhosseini, A. (2014). Biomechanical properties of native and tissue engineered heart valve constructs. Journal of Biomechanics, 47(9), 1949–1963. https://doi.org/10.1016/j.jbiomech.2013.09.023

Heidari, F., Bahrololoom, M. E., Vashaee, D., & Tayebi, L. (2015). In situ preparation of iron oxide nanoparticles in natural hydroxyapatite/chitosan matrix for bone tissue engineering application. Ceramics International, 41(2), 3094–3100. https://doi.org/10.1016/j.ceramint.2014.10.153

Hinck, A. P., Mueller, T. D., & Springer, T. A. (2016). Structural Biology and Evolution of the TGF-β Family. Cold Spring Harbor Perspectives in Biology, 8(12), a022103. https://doi.org/10.1101/cshperspect.a022103

Hockaday, L. A., Kang, K. H., Colangelo, N. W., Cheung, P. Y. C., Duan, B., Malone, E., Wu, J., Girardi, L. N., Bonassar, L. J., Lipson, H., Chu, C. C., & Butcher, J. T. (2012). Rapid 3D printing of anatomically accurate and mechanically heterogeneous aortic valve hydrogel scaffolds. Biofabrication, 4(3), 035005. https://doi.org/10.1088/1758-5082/4/3/035005

Huang, Z.-M., Zhang, Y.-Z., Kotaki, M., & Ramakrishna, S. (2003). A review on polymer nanofibers by electrospinning and their applications in nanocomposites. Composites Science and Technology, 63(15), 2223–2253. https://doi.org/10.1016/S0266-3538(03)00178-7

Jana, S., Tefft, B. J., Spoon, D. B., & Simari, R. D. (2014). Scaffolds for tissue engineering of cardiac valves. Acta Biomaterialia, 10(7), 2877–2893. https://doi.org/10.1016/j.actbio.2014.03.014

Khaki, M., Salmanian, A. H., Abtahi, H., Ganji, A., & Mosayebi, G. (2018). Mesenchymal Stem Cells Differentiate to Endothelial Cells Using Recombinant Vascular Endothelial Growth Factor –A. Reports of Biochemistry & Molecular Biology, 6(2), 144. /pmc/articles/PMC5940356/

LANGER, R., & FOLKMAN, J. (1976). Polymers for the sustained release of proteins and other macromolecules. Nature, 263(5580), 797–800. https://doi.org/10.1038/263797a0

Langer Vacanti J. P., R. (1993). Tissue engineering. Science, 260(5110), 920–926. https://doi.org/10.1126/science.8493529

Lanuti, P., Rotta, G., Almici, C., Avvisati, G., Budillon, A., Doretto, P., Malara, N., Marini, M., Neva, A., Simeone, P., Di Gennaro, E., Leone, A., Falda, A., Tozzoli, R., Gregorj, C., Di Cerbo, M., Trunzo, V., Mollace, V., Marchisio, M., & Miscia, S. (2016). Endothelial progenitor cells, defined by the simultaneous surface expression of <scp>VEGFR</scp> 2 and <scp>CD</scp> 133, are not detectable in healthy peripheral and cord blood. Cytometry Part A, 89(3), 259–270. https://doi.org/10.1002/cyto.a.22730

Li, X. P., Li, Y., Li, X., Song, D., Min, P., Hu, C., Zhang, H. Bin, Koratkar, N., & Yu, Z. Z. (2019). Highly sensitive, reliable and flexible piezoresistive pressure sensors featuring polyurethane sponge coated with MXene sheets. Journal of Colloid and Interface Science, 542, 54–62. https://doi.org/10.1016/J.JCIS.2019.01.123

Loshusan et al., B. R. (2024). The Ross procedure for recurrently failed aortic valve procedures. Multimedia Manual of Cardiothoracic Surgery. https://doi.org/10.1510/mmcts.2024.0249

Massagué, J. (2012). TGFβ signalling in context. Nature Reviews Molecular Cell Biology, 13(10), 616–630. https://doi.org/10.1038/nrm3434

Mendoza et al., J. C. (2024). Management of surgical aortic valve replacement degeneration with transcatheter aortic valve implantation (TAVI): Experience in Nicaragua. Cureus. https://doi.org/10.7759/cureus.13905

Min and Cho S. W., S. (2022). Engineered human cardiac tissues for modeling heart diseases. BMB Reports. https://doi.org/10.5483/BMBRep.2022.55.2.210

Mizuno, H. (2009). Adipose-derived stem cells for tissue repair and regeneration: Ten years of research and a literature review. Journal of Nippon Medical School, 76(2), 56–66. https://doi.org/10.1272/jnms.76.56

Mosch, J., Gleissner, C. A., Body, S., & Aikawa, E. (2017). Histopathological assessment of calcification and inflammation of calcific aortic valves from patients with and without diabetes mellitus. Histology and Histopathology, 32(3), 293–306. https://doi.org/10.14670/HH-11-797

Motta et al., S. E. (2021). Pluripotent stem cell applications in cardiovascular tissue engineering. Stem Cell Reports. https://doi.org/10.1016/j.stemcr.2021.03.019

Murphy, S. V, & Atala, A. (2014). 3D bioprinting of tissues and organs. Nature Biotechnology, 32(8), 773–785. https://doi.org/10.1038/nbt.2958

Murphy Wang H. T. Nguyen T., M. P. (2020). Mesenchymal stem cells and their role in tissue engineering. Nature Reviews Materials, 5(3), 149–161. https://doi.org/10.1038/s41578-020-0197-7

Nuche et al., J. (2024). Transcatheter aortic valve replacement in aortic stenosis patients with NYHA functional class III or IV. Canadian Journal of Cardiology. https://doi.org/10.1016/j.cjca.2023.09.004

O'Brien, F. J. (2011). Biomaterials & scaffolds for tissue engineering. Materials Today, 14(3), 88–95. https://doi.org/10.1016/S1369-7021(11)70058-X

Ovcharenko, E. A., Klyshnikov, K. U., Vlad, A. R., Sizova, I. N., Kokov, A. N., Nushtaev, D. V., Yuzhalin, A. E., & Zhuravleva, I. U. (2014). Computer-aided design of the human aortic root. Computers in Biology and Medicine, 54, 109–115. https://doi.org/10.1016/j.compbiomed.2014.08.023

Patil et al., P. S. (2019). Oxygen regulation in development: Lessons from embryogenesis towards tissue engineering. Cells Tissues Organs. https://doi.org/10.1159/000503162

Petreaca, M., & Martins-Green, M. (2020). The dynamics of cell–extracellular matrix interactions, with implications for tissue engineering. In Principles of Tissue Engineering (pp. 93–117). Elsevier. https://doi.org/10.1016/B978-0-12-818422-6.00007-1

Rendon-Romero et al., L. M. (2024). Advances in dynamic bioreactors for tissue engineering. Tissue Engineering Part B: Reviews. https://doi.org/10.1089/ten.teb.2024.0227

Richardson, T. P., Peters, M. C., Ennett, A. B., & Mooney, D. J. (2001). Polymeric system for dual growth factor delivery. Nature Biotechnology, 19(11), 1029–1034. https://doi.org/10.1038/nbt1101-1029

Rieder, E., Kasimir, M.-T., Silberhumer, G., Seebacher, G., Wolner, E., Simon, P., & Weigel, G. (2004). Decellularization protocols of porcine heart valves differ importantly in efficiency of cell removal and susceptibility of the matrix to recellularization with human vascular cells. The Journal of Thoracic and Cardiovascular Surgery, 127(2), 399–405. https://doi.org/10.1016/j.jtcvs.2003.06.017

Saidy, N. T., Wolf, F., Bas, O., Keijdener, H., Hutmacher, D. W., Mela, P., & De-Juan-Pardo, E. M. (2019). Biologically Inspired Scaffolds for Heart Valve Tissue Engineering via Melt Electrowriting. Small, 15(24). https://doi.org/10.1002/smll.201900873

Schiele, N. R., Corr, D. T., Huang, Y., Raof, N. A., Xie, Y., & Chrisey, D. B. (2010). Laser-based direct-write techniques for cell printing. Biofabrication, 2(3), 032001. https://doi.org/10.1088/1758-5082/2/3/032001

Schumacher et al., A. (2018). In vitro antimicrobial susceptibility testing methods: Agar dilution to 3D tissue-engineered models. European Journal of Clinical Microbiology & Infectious Diseases. https://doi.org/10.1007/s10096-017-3089-2

Sewell-Loftin, M. K., Chun, Y. W., Khademhosseini, A., & Merryman, W. D. (2011). EMT-Inducing Biomaterials for Heart Valve Engineering: Taking Cues from Developmental Biology. Journal of Cardiovascular Translational Research, 4(5), 658–671. https://doi.org/10.1007/s12265-011-9300-4

Sodian, R., Hoerstrup, S. P., Sperling, J. S., Daebritz, S., Martin, D. P., Moran, A. M., Kim, B. S., Schoen, F. J., Vacanti, J. P., & Mayer, J. E. (2000). Early In Vivo Experience With Tissue-Engineered Trileaflet Heart Valves. Circulation, 102(Supplement 3), III-22-III–29. https://doi.org/10.1161/01.CIR.102.suppl_3.III-22

Takahashi Yamanaka S., K. (2006). Induction of pluripotent stem cells from mouse embryonic and adult fibroblast cultures by defined factors. Cell, 126(4), 663–676. https://doi.org/10.1016/j.cell.2006.07.024

Teo, W. E., & Ramakrishna, S. (2006). A review on electrospinning design and nanofibre assemblies. Nanotechnology, 17(14), R89–R106. https://doi.org/10.1088/0957-4484/17/14/R01

Thomson et al., J. A. (1998). Embryonic stem cell lines derived from human blastocysts. Science, 282(5391), 1145–1147. https://doi.org/10.1126/science.282.5391.1145

Varghese, R., Salvi, S., Sood, P., Karsiya, J., & Kumar, D. (2022). Recent advancements in additive manufacturing techniques employed in the pharmaceutical industry: A bird's eye view. Annals of 3D Printed Medicine, 8, 100081. https://doi.org/10.1016/j.stlm.2022.100081

Weber, J. F., Perez, R., & Waldman, S. D. (2015). Mechanobioreactors for Cartilage Tissue Engineering (pp. 203–219). https://doi.org/10.1007/978-1-4939-2938-2_15

Weissman, I. L. (2000). Stem cells: Units of development, units of regeneration, and units in evolution. Cell, 100(1), 157–168. https://doi.org/10.1016/S0092-8674(00)81692-X

Wells et al., S. M. (2021). Biomechanical conditioning of tissue-engineered constructs: Current trends. Journal of Biomedical Materials Research. https://doi.org/10.1002/jbm.a.37348

Wu, J., Brazile, B., McMahan, S. R., Liao, J., & Hong, Y. (2019). Heart valve tissue-derived hydrogels: Preparation and characterization of mitral valve chordae, aortic valve, and mitral valve gels. Journal of Biomedical Materials Research Part B: Applied Biomaterials, 107(5), 1732–1740. https://doi.org/10.1002/jbm.b.34266

Xu et al., Y. (2022). Development of advanced bioreactor systems for tissue-engineered heart valves. Biomaterials. https://doi.org/10.1016/j.biomaterials.2021.120869

Yacoub, M. H., & Takkenberg, J. J. M. (2005). Will heart valve tissue engineering change the world? Nature Clinical Practice Cardiovascular Medicine, 2(2), 60–61. https://doi.org/10.1038/ncpcardio0112

Yadid, M., Oved, H., Silberman, E., & Dvir, T. (2022). Bioengineering approaches to treat the failing heart: from cell biology to 3D printing. Nature Reviews Cardiology, 19(2), 83–99. https://doi.org/10.1038/s41569-021-00603-7

Yang et al., F. (2022). In situ tissue engineering for heart valves: A regenerative approach. ACS Biomaterials Science & Engineering. https://doi.org/10.1021 /acsbiomaterials. 2c01199

Yilgor, P., Tuzlakoglu, K., Reis, R. L., Hasirci, N., & Hasirci, V. (2009). Incorporation of a sequential BMP-2/BMP-7 delivery system into chitosan-based scaffolds for bone tissue engineering. Biomaterials, 30(21), 3551–3559. https://doi.org/10.1016/j.biomaterials.2009.03.024

Zaimi et al., I. (2024). Advances in tissue engineering and regenerative medicine: A systematic review. Applied Sciences. https://doi.org/10.3390/app14120633

Zhang, Y., Ouyang, H., Lim, C. T., Ramakrishna, S., & Huang, Z. (2005). Electrospinning of gelatin fibers and gelatin/PCL composite fibrous scaffolds. Journal of Biomedical Materials Research Part B: Applied Biomaterials, 72B(1), 156–165. https://doi.org/10.1002/jbm.b.30128

Zhu and Yang L., Z. (2024). Advances in molecular diagnostics: Tissue engineering applications. TrAC Trends in Analytical Chemistry. https://doi.org/10.1016/ j.trac.2024.103856

Zuk et al., P. A. (2001). Multilineage cells from human adipose tissue: Implications for cell-based therapies. Tissue Engineering, 7(2), 211–228. https://doi.org/10. 1089/107632701300062859

APPENDICES

Absorbance Values and Standard Curves of ELISA Tests

User: USER
Path: C:\Program Files\BMG\CLARIOstar\User\Data\
Test ID: 818
Test Name: eliza450-pınar
Date: 04.01.2025
Time: 18:11:24
Absorbance — Absorbance values are displayed as OD

Raw Data (450)

	1	2	3	4	5	6	7	8	9	10	11	12
A	3,5	1,357	0,32	0,249	0,25	0,001	0,001	0,001	0,0008	0,001	0,0007	0,0009
B	3,5	1,236	0,218	0,223	0,28	0,001	0,0009	0,001	0,0008	0,0007	0,0009	0,0009
C	3,5	0,74	0,235	0,226	0,278	0,001	0,001	0,001	0,001	0,001	0,001	0,001
D	3,404	0,744	0,226	0,232	0,245	0,001	0,001	0,0009	0,0009	0,001	0,001	0,001
E	3,214	0,525	0,238	0,212	0,182	0,001	0,0007	0,0009	0,0008	0,001	0,001	0,0009
F	3,232	0,447	0,246	0,236	0,169	0,001	0,0009	0,0009	0,001	0,0009	0,001	0,0008
G	2,214	0,227	0,214	0,229	0,192	0,001	0,001	0,0009	0,001	0,0009	0,001	0,001
H	2,203	0,195	0,183	0,195	0,195	0,001	0,001	0,001	0,001	0,001	0,001	0,001

Standarts

Samples

TGF-B1 Elisa absorbance values

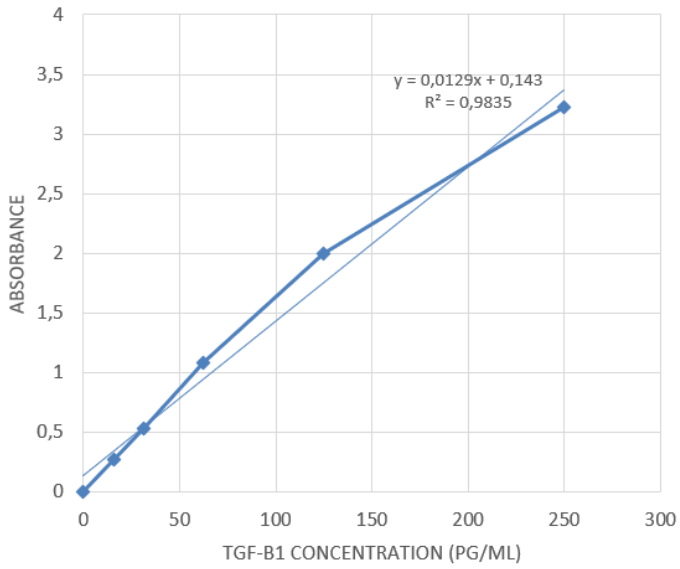

TGF-B1 standard curve for ELISA

User: USER
Path: C:\Program Files\BMG\CLARIOstar\User\Data\
Test ID: 817
Test Name: eliza450-pınar
Date: 04.01.2025
Time: 18:03:06
Absorbance — Absorbance values are displayed as OD

Raw Data (450)

	1	2	3	4	5	6	7	8	9	10	11	12
A	3,5	1,226	0,281	0,226	0,228	0,001	0,001	0,001	0,001	0,001	0,002	0,002
B	3,5	1,219	0,236	0,208	0,251	0,002	0,002	0,002	0,002	0,001	0,002	0,001
C	3,489	0,644	0,253	0,198	0,239	0,002	0,002	0,002	0,002	0,002	0,002	0,002
D	3,444	0,612	0,241	0,256	0,21	0,002	0,002	0,002	0,002	0,002	0,002	0,002
E	2,642	0,39	0,2	0,199	0,25	0,002	0,002	0,002	0,002	0,002	0,002	0,002
F	2,607	0,375	0,199	0,187	0,232	0,002	0,002	0,002	0,002	0,002	0,002	0,002
G	1,763	0,203	0,197	0,213	0,209	0,002	0,002	0,002	0,002	0,002	0,002	0,002
H	1,541	0,185	0,206	0,215	0,25	0,002	0,002	0,002	0,002	0,002	0,002	0,002

Standarts

Samples

VEGF Elisa absorbance values

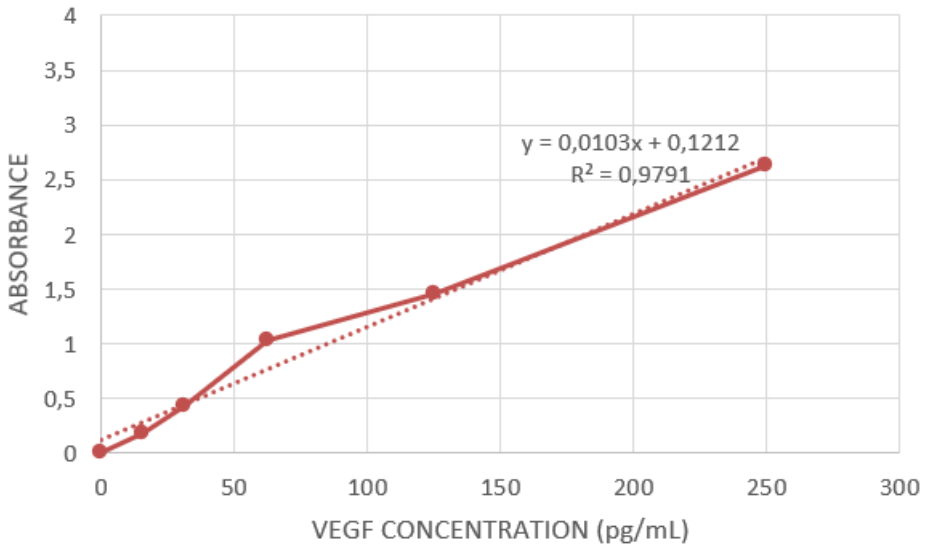

VEGF standard curve for ELISA